Journal of Asian Earth Sciences 58 (2012) 64–77

Contents lists available at SciVerse ScienceDirect

Journal of Asian Earth Sciences

journal homepage: www.elsevier.com/locate/jseaes

Major and trace elements of a peat core from Yunnan, Southwest China: Implications for paleoclimatic proxies

Gangjian Wei [a,*], Luhua Xie [b], Yongge Sun [c], Yuehan Lu [c], Ying Liu [a]

[a] State Key Laboratory of Isotope Geochemistry, Guangzhou Institute of Geochemistry, Chinese Academy of Sciences, Guangzhou 510640, China
[b] Key Laboratory of Marginal Sea Geology, Guangzhou Institute of Geochemistry, Chinese Academy of Sciences, Guangzhou 510640, China
[c] State Key Laboratory of Organic Geochemistry, Guangzhou Institute of Geochemistry, Chinese Academy of Sciences, Guangzhou 510640, China

ARTICLE INFO

Article history:
Received 16 June 2011
Received in revised form 25 April 2012
Accepted 22 June 2012
Available online 20 July 2012

Keywords:
Peats
Major and trace elements
Chemical weathering
East Asian summer monsoon

ABSTRACT

This study examines the accumulation of major and trace elements in peat deposits in central Yunnan Province, southwestern China. The ashes of an approximately 2 m long core spanning 32.7–11.4 ka are analyzed to assess the elemental contributions of organic materials and to identify elemental paleoclimatic proxies in peats. Peat ash, which is mainly composed of silicate materials, makes up 20–80% of each of the samples. The analysis shows that organic materials are a significant source of many of the elements in the ashes. Among these elements, P and V are the most typical, with their concentrations in the ashes closely correlating to the total organic carbon (TOC) content of the peats. Al, Na, Sc, Cr, Co, Ni, Cu, Ge, Pb, and Th are also associated with biogenic materials, particularly in the lower section (below 122 cm) of the core, where the organic material content is high. Ca, Sr, Mg, and Mn appear to have been part of carbonate deposits, such as authigenic $FeCO_3$ and $MnCO_3$ in the anoxic peats, whereas, K, Ti, Zn, Ga, Rb, Y, rare earth elements (REEs), Zr, Hf, Nb, Ta, Ba, and U are mainly associated with silicate materials. Local weathering products, rather than dust from northern China, are the main sources for the silicate materials in these peats. Some elemental ratios such as K/Rb and K_2O/Na_2O can reliably indicate changes in local chemical weathering intensity, and their variation patterns match the changes in the East Asian summer monsoon (EASM) very well. The less intensive chemical weathering indicated by lower K/Rb and K_2O/Na_2O ratios generally corresponds to weaker EASM strength during ~30 to ~10 ka, which is consistent with the fact that weaker summer monsoons may arouse drier climates, and do not favor intense chemical weathering. This suggests that select elemental ratios in peats/organic rich sediments may be informative proxies for monsoon climate changes.

1. Introduction

Peats are valuable archives of climate and environment changes, and proxies in peats have been used to reconstruct paleoclimatic and paleoenvironmental records for more than a century (Bindler, 2006). Most of these proxies are associated with biogenic materials, such as pollen, peat-forming fossils, elements and isotopes of organic matter, and some newly developed molecular biomarkers (Bindler, 2006). Inorganic materials in peats, however, can also provide plentiful information about climate and environment changes. In ombrotrophic peat bogs, inorganic materials are believed to be mainly atmospheric deposits, and their elemental and isotopic compositions probably indicate changes in atmospheric inputs. Numerous studies in the past decades have described the changes in atmospheric imported heavy metals, such as lead and mercury, during industrial eras or during pre-industrial periods in Europe and North America (Farmer et al., 2006; Kamenov et al., 2009; Kempter et al., 1997; Kylander et al., 2005, 2007; Le Roux et al., 2004; Martinez-Cortizas et al., 1999, 2002; Roos-Barraclough et al., 2002; Shotyk et al., 1998, 2001, 2005; Weiss et al., 1997, 1999). These studies of natural and anthropogenic inputs from the atmosphere are important in the evaluation of the impact of human activities on the environment. The geochemistry of inorganic materials in minerotrophic peat bogs are also believed to be informative proxies for climate and environment changes, even though inorganic materials carried by water flow can conceal materials imported from the atmosphere. Not only human activities (Monna et al., 2004a,b), but also natural climate changes (Kylander et al., 2007; Muller et al., 2006, 2008) can be reflected in the elemental and isotopic compositions of the inorganic materials in minerotrophic peat bogs.

Peat can generally be considered as a special type of sediment comprising a large amount of biogenic materials transformed from

* Corresponding author. Address: 511 Kehua Rd., Guangzhou Institute of Geochemistry, CAS, Guangzhou 510640, China. Tel.: +86 20 85290093; fax: +86 20 85290130.
E-mail address: gjwei@gig.ac.cn (G. Wei).

1367-9120/$ - see front matter © 2012 Elsevier Ltd. All rights reserved.
http://dx.doi.org/10.1016/j.jseaes.2012.06.021

Table 1
LOI and TOC contents of the peats and the major element contents of the ashes (unit: %).

Sample ID	Depth (cm)	Age (ka)	LOI	TOC	Al_2O_3	CaO	FeO(T)[a]	K_2O	MgO	MnO	Na_2O	P_2O_5	TiO_2
BX-21	42	11.42	21.84	6.92	27.22	2.02	4.95	3.07	1.19	0.03	0.18	0.06	0.90
BX-22	44	11.84	20.63	6.64	26.95	1.87	4.90	3.09	1.19	0.03	0.16	0.06	0.96
BX-23	46	12.26	30.14	11.38	28.49	3.67	6.67	2.62	1.39	0.05	0.19	0.12	0.88
BX-24	48	12.68	28.33	8.94	28.82	2.87	5.96	2.80	1.31	0.03	0.15	0.10	0.90
BX-25	50	13.10	30.95	11.33	28.64	3.03	6.09	2.76	1.35	0.04	0.18	0.11	0.89
BX-26	52	13.51	34.81	14.02	26.54	3.77	6.01	2.56	1.43	0.04	0.27	0.16	0.90
BX-27	54	13.93	38.24	16.84	23.89	4.02	6.69	2.34	1.33	0.06	0.27	0.20	0.88
BX-28	56	14.35	38.61	15.60	23.52	3.97	7.14	2.36	1.34	0.06	0.25	0.24	0.93
BX-29	58	14.77	40.29	16.79	24.33	4.33	7.69	2.49	1.45	0.06	0.26	0.30	0.97
BX-30	60	15.19	44.60	20.17	25.67	4.67	7.06	2.48	1.46	0.05	0.24	0.27	0.89
BX-31	62	15.61	47.40	21.79	26.93	4.85	7.38	2.61	1.51	0.05	0.20	0.31	0.89
BX-32	64	16.03	45.14	19.96	27.65	4.09	6.29	2.78	1.46	0.04	0.18	0.25	0.93
BX-33	66	16.45	46.39	23.28	27.29	4.05	5.48	2.65	1.53	0.03	0.22	0.30	0.94
BX-34	68	16.87	45.50	22.16	26.10	3.21	5.53	2.61	1.37	0.03	0.22	0.29	0.97
BX-35	70	17.29	48.19	21.26	24.99	3.61	5.82	2.39	1.34	0.03	0.27	0.38	0.98
BX-36	72	17.71	50.21	24.63	24.69	3.88	5.34	2.18	1.34	0.03	0.32	0.43	0.96
BX-37	74	18.13	50.93	24.35	24.19	3.81	5.40	2.07	1.30	0.03	0.29	0.45	0.93
BX-38	76	18.38	52.76	25.46	24.98	3.96	5.31	2.03	1.36	0.03	0.29	0.50	0.93
BX-39	78	18.85	51.66	25.55	25.19	3.81	5.08	2.09	1.38	0.03	0.32	0.46	0.93
BX-40	80	19.31	50.03	24.56	24.80	3.21	4.94	2.11	1.30	0.03	0.29	0.41	0.93
BX-41	82	19.78	47.98	23.39	24.20	2.85	4.69	2.11	1.24	0.03	0.28	0.39	0.90
BX-42	84	20.24	49.83	23.76	25.32	3.07	4.89	2.28	1.33	0.03	0.27	0.36	0.92
BX-43	86	20.71	51.70	25.63	25.77	3.10	4.95	2.31	1.33	0.03	0.26	0.37	0.90
BX-44	88	21.18	43.31	20.96	26.74	2.63	5.08	2.56	1.30	0.03	0.23	0.31	0.89
BX-45	90	21.64	43.95	18.93	27.05	2.55	4.89	2.70	1.30	0.03	0.23	0.29	0.89
BX-46	92	22.11	41.13	18.64	25.72	2.28	4.82	2.68	1.21	0.03	0.22	0.29	0.89
BX-47	94	22.57	41.44	19.88	26.65	2.35	4.81	2.86	1.25	0.03	0.23	0.27	0.93
BX-48	96	23.04	38.18	18.83	26.95	2.28	4.48	3.11	1.30	0.02	0.21	0.22	0.91
BX-49	98	23.42	35.67	16.51	26.61	1.85	4.33	3.39	1.23	0.02	0.18	0.17	0.95
BX-50	100	23.81	38.18	18.42	26.46	2.15	4.40	3.24	1.28	0.02	0.19	0.20	0.89
BX-51	102	24.19	39.55	19.77	26.29	2.01	4.17	3.24	1.25	0.03	0.18	0.16	0.92
BX-52	104	24.57	44.44	22.17	26.80	2.53	4.43	3.12	1.37	0.03	0.19	0.19	0.87
BX-53	106	24.95	51.27	25.21	26.15	2.36	4.62	3.12	1.32	0.03	0.19	0.20	0.87
BX-54	108	25.34	50.92	25.91	27.28	2.44	4.50	3.26	1.41	0.03	0.19	0.21	0.83
BX-55	110	25.72	47.99	24.56	26.30	2.02	4.25	3.49	1.29	0.03	0.18	0.18	0.83
BX-56	112	26.10	42.36	21.58	26.81	1.73	4.20	3.77	1.28	0.02	0.17	0.16	0.87
BX-57	114	26.48	44.32	19.80	26.91	1.71	4.14	3.66	1.31	0.02	0.18	0.16	0.86
BX-58	116	26.87	41.44	20.84	26.05	1.31	3.87	3.82	1.25	0.02	0.17	0.12	0.87
BX-59	118	27.25	41.38	19.53	25.88	1.36	3.95	3.79	1.25	0.02	0.17	0.14	0.83
BX-60	120	27.63	51.16	25.55	27.29	2.11	4.64	3.51	1.43	0.03	0.20	0.21	0.84
BX-61	122	27.68	57.18	29.67	26.06	3.13	5.69	2.90	1.48	0.04	0.21	0.32	0.80
BX-62	124	27.74	56.29	29.14	26.62	3.62	6.13	2.87	1.61	0.05	0.22	0.35	0.80
BX-63	126	27.79	63.76	33.39	26.69	3.69	6.68	2.68	1.56	0.05	0.23	0.39	0.79
BX-64	128	27.84	73.81	35.19	27.41	4.27	6.65	2.50	1.70	0.05	0.25	0.40	0.80
BX-65	130	27.90	70.33	37.98	27.61	3.83	6.76	2.44	1.56	0.05	0.23	0.41	0.81
BX-66	132	27.95	59.47	39.83	27.86	3.81	6.76	2.48	1.66	0.05	0.25	0.42	0.79
BX-67	134	28.00	70.52	40.40	27.86	3.68	6.95	2.60	1.68	0.05	0.27	0.44	0.82
BX-68	136	28.06	80.43	44.46	27.46	3.87	7.34	2.46	1.69	0.05	0.27	0.49	0.84
BX-69	138	28.11	66.21	35.35	26.98	2.87	6.29	2.87	1.45	0.04	0.23	0.32	0.88
BX-70	140	28.16	61.14	31.90	26.44	2.78	5.98	2.83	1.40	0.04	0.20	0.30	0.88
BX-71	142	28.22	57.21	29.88	26.68	2.85	5.95	2.89	1.40	0.04	0.21	0.29	0.87
BX-72	144	28.27	62.73	40.51	25.35	2.99	6.36	2.70	1.38	0.04	0.22	0.30	0.87
BX-73	146	28.32	52.94	26.81	26.27	3.05	6.02	2.99	1.42	0.05	0.19	0.26	0.90
BX-74	148	28.38	49.86	24.41	23.92	3.25	6.39	2.43	1.31	0.05	0.19	0.25	0.89
BX-75	150	28.43	50.61	25.63	23.20	3.47	6.31	2.38	1.34	0.05	0.19	0.26	0.91
BX-76	152	28.48	49.66	26.00	24.13	3.49	6.47	2.61	1.41	0.05	0.18	0.25	0.92
BX-77	154	28.54	51.52	25.69	24.09	2.71	5.83	2.60	1.27	0.04	0.17	0.22	0.95
BX-78	156	28.59	50.14	25.57	22.46	2.25	5.23	2.66	1.22	0.04	0.16	0.20	0.96
BX-79	158	28.64	50.32	25.61	25.34	2.01	4.99	3.10	1.29	0.03	0.16	0.19	1.00
BX-80	160	28.70	48.07	25.30	25.06	1.84	4.80	3.13	1.26	0.03	0.16	0.18	1.00
BX-81	162	28.75	42.99	21.45	25.15	1.36	4.39	3.20	1.20	0.02	0.16	0.15	1.05
BX-82	164	28.96	40.95	19.53	25.08	1.10	3.87	3.36	1.17	0.02	0.15	0.13	1.03
BX-83	166	29.17	55.59	29.93	25.65	1.49	4.54	3.22	1.25	0.02	0.17	0.17	1.01
BX-84	168	29.37	46.97	23.59	25.33	1.30	4.24	3.26	1.20	0.02	0.15	0.14	1.02
BX-85	170	29.58	49.31	25.70	25.65	1.34	4.22	3.36	1.25	0.02	0.15	0.14	1.02
BX-86	172	29.79	43.41	21.80	24.90	1.10	4.08	3.30	1.21	0.02	0.15	0.11	1.03
BX-87	174	30.00	46.35	23.44	25.45	1.16	4.23	3.39	1.25	0.02	0.16	0.12	1.05
BX-88	176	30.20	41.44	21.69	25.46	1.06	3.92	3.41	1.24	0.02	0.14	0.11	1.02
BX-89	178	30.41	42.86	21.17	26.17	1.10	4.20	3.52	1.27	0.02	0.16	0.11	1.08
BX-90	180	30.62	41.79	20.86	25.52	1.09	4.03	3.40	1.24	0.02	0.14	0.10	1.02
BX-91	182	30.83	40.17	19.69	24.76	1.02	4.00	3.21	1.19	0.02	0.14	0.10	1.01
BX-92	184	31.03	39.26	18.45	25.11	1.04	4.04	3.23	1.20	0.02	0.14	0.10	1.01
BX-93	186	31.24	39.97	19.63	22.42	1.03	4.10	3.10	1.09	0.02	0.14	0.10	0.99
BX-94	188	31.45	51.39	26.49	26.46	1.47	4.70	3.17	1.32	0.03	0.16	0.15	0.94

(*continued on next page*)

Table 1 (*continued*)

Sample ID	Depth (cm)	Age (ka)	LOI	TOC	Al_2O_3	CaO	FeO(T)[a]	K_2O	MgO	MnO	Na_2O	P_2O_5	TiO_2
BX-95	190	31.66	48.46	24.16	26.58	1.63	5.11	3.05	1.29	0.03	0.16	0.15	0.95
BX-96	192	31.86	50.14	24.68	26.45	1.77	5.41	2.90	1.31	0.03	0.17	0.16	0.92
BX-97	194	32.07	52.75	27.27	26.87	1.93	5.61	2.96	1.38	0.03	0.17	0.18	0.92
BX-98	196	32.28	56.24	27.73	26.08	2.09	6.07	2.78	1.35	0.04	0.18	0.20	0.91
BX-100	200	32.70	60.42	32.96	25.92	1.82	7.14	2.79	1.30	0.03	0.18	0.23	0.90

[a] FeO(T): total Fe.

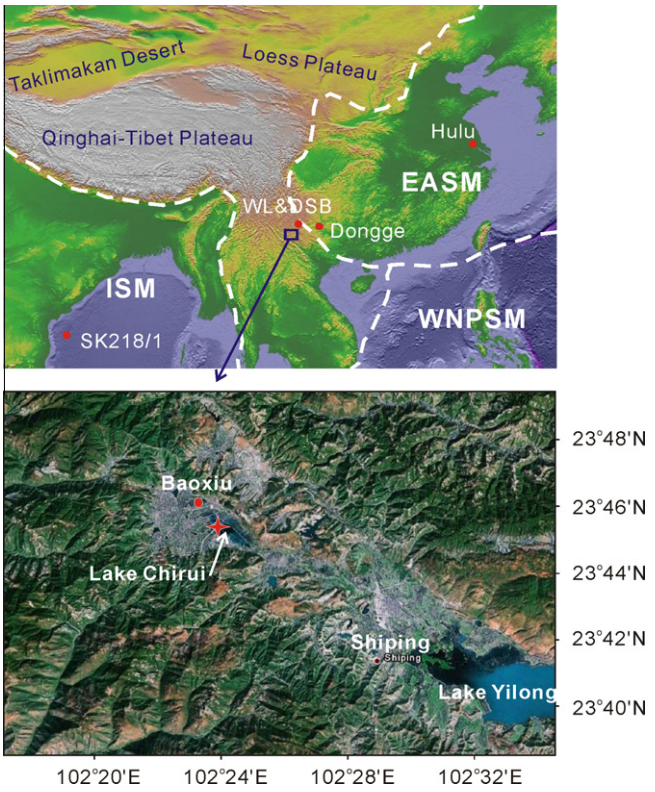

Fig. 1. Location of Chirui Lake. The dashed lines outline the regions influenced by the three branches of the East Asian summer monsoon: EASM, East Asian summer monsoon; ISM, Indian summer monsoon; and WNPSM, Western North Pacific summer monsoon. The terms of the summer monsoon branches and their influence in various regions are from Wang and Lin (2002). The locations of the paleoclimate records included in the discussion, such as Hulu, Dongge, Wulu and Dashibao (WL&DSB) caves, and the core SK218/1 are also shown on the map.

plants; the redox condition in peats is extremely anoxic or euxinic. Plants generally accumulate some metals from the soil, and a high concentration of these metals in the phytoliths may significantly influence the composition of the peats (Wust and Bustin, 2003). Such plant-derived metals are different from those in the inorganic materials input from the atmosphere or carried by water flow, and they may bias paleoclimatic interpretations of peats (Wust and Bustin, 2003). However, the extent to which the plant-derived metals contribute to the total metal concentrations in peats, and how they influence the paleoclimatic records is still not well known. It is apparent that such influences need to be assessed before appropriate elemental proxies for paleoclimatic change can be identified.

Here, we report the major and trace elements in the peats/sediments of an approximately 2 m peat core collected from Baoxiu Basin in the central Yunnan Province, southwestern China. The samples from this core, comprised of peats and organic rich sediments, have total organic carbon (TOC) contents ranging from 6.64% to 44.46% (Lu, 2003). The large variation in the organic material contents is helpful in the evaluation of their contribution to the major and trace element concentrations in peats. The correlation between elements and organic materials is discussed in detail below and the contribution of biogenic materials to the major and trace elements in peats is assessed. Moreover, several typical proxies for chemical weathering are compared to evaluate the influence of plant-derived elements on the paleoclimatic records. This analysis provides a better understand of the behaviors of elements in peats, enabling us to clarify the relationships between the elements, and climatic and environmental changes. The results of this work will improve reconstruction of paleoclimatic records using peats.

2. Materials and methods

2.1. Site description

Baoxiu Basin (23°46′N, 102°23′E) is located in Shiping County in the central Yunnan Province, southwestern China (Fig. 1). The altitude of this basin is 1400–1430 m, and the mountains to its south, west, and north have altitudes of 1500–2000 m. Streams originating from the surrounding mountains flow into Chirui Lake, located in the center of Baoxiu Basin, and the water flows southeast out of Chirui Lake into Yilong Lake. Chirui Lake is 0.5–1.0 km^2 in size, with water depths of 1–3 m. These depths vary between the rainy and dry seasons.

Baoxiu Basin is very close to the boundary of the region controlled by the East Asian summer monsoon (EASM) (Wang and Lin, 2002), as shown in Fig. 1. The climate in this region is very sensitive to changes in the EASM. It is a sub-tropical region, with an annual temperature and precipitation of about 18 °C and 960 mm, respectively. About 80% of the precipitation in this region occurs during the rainy season from May to October, when the summer monsoon prevails.

Peat is deposited around Chirui Lake, and grass was the dominant plant that formed these peats.

2.2. Samples and experiments

A 200 cm long core was collected from the margin of Chirui Lake. The sample was taken from above the seasonal variation range of the water level. Disturbance was observed in the top 40 cm of the core, which may be attributed to farming around the lake prior to the 1970s. The peat core was divided into samples at 2 cm intervals in the field and packed into plastic bags.

Samples for geochemical measurement were freeze-dried, hand-milled using a mortar, and then sieved through a 250 μm sieve. The pre-treated samples were precisely weighed into clean porcelain vials, and baked at 900 °C for 2 h to measure loss on ignition (LOI). The ash was collected for further elemental measurement, and all of the element concentrations were measured relative to the ash. Samples from the top 40 cm of soil were not included in further geochemical measurements.

Table 2
Trace element concentrations of the ashes (unit: ppm).

ID	BX-21	BX-22	BX-23	BX-24	BX-25	BX-26	BX-27	BX-28	BX-29	BX-30	BX-31	BX-32	BX-33	BX-34
Depth (cm)	42	44	46	48	50	52	54	56	58	60	62	64	66	68
Age (ka)	11.42	11.84	12.26	12.68	13.10	13.51	13.93	14.35	14.77	15.19	15.61	16.03	16.45	16.87
Sc	31.3	31.3	32.9	32.2	31.8	30.2	28.7	28.6	30.2	31.8	32.3	32.2	32.1	31.3
V	198	193	233	215	211	194	202	208	216	228	249	236	224	228
Cr	144	141	167	152	150	159	141	145	156	156	151	151	165	147
Co	22.2	21.3	25.7	24.5	25.0	24.2	25.1	25.2	23.3	25.2	24.2	22.9	21.2	22.4
Ni	57.3	55.0	67.2	66.6	67.5	67.8	66.2	69.0	70.4	76.2	75.3	74.1	73.9	71.3
Cu	82.0	85.8	122	105	105	97.4	81.2	80.5	91.5	105	104	103	139	148
Zn	72.1	90.6	95.3	116.2	114.0	91.0	85.7	85.5	77.2	90.8	97.1	99.3	88.7	98.9
Ga	36.2	37.1	38.0	39.0	39.8	35.4	33.1	33.4	32.3	34.9	35.2	37.5	36.4	37.0
Ge	3.49	3.65	3.73	4.07	4.25	3.86	3.46	3.42	3.43	3.90	3.98	4.19	3.66	3.68
Rb	230	240	219	241	231	211	208	202	206	230	241	246	214	213
Sr	67.9	62.3	92.1	78.2	81.0	96.1	105	102	104	114	115	99.5	96.0	83.8
Y	41.5	43.9	43.4	43.3	42.2	40.6	40.3	43.5	41.3	42.5	44.5	43.7	42.1	42.7
Zr	227	213	208	205	202	203	196	191	193	206	204	214	201	210
Nb	17.6	18.8	16.9	16.6	16.4	17.3	16.5	16.7	17.3	16.3	16.4	17.1	17.7	17.6
Ba	712	695	702	686	677	672	656	668	655	676	680	663	645	641
La	57.0	58.6	59.9	59.1	58.1	53.6	53.7	52.6	52.0	56.5	57.9	55.4	54.1	53.5
Ce	139	136	149	139	135	131	126	124	126	135	141	132	129	125
Pr	13.6	14.1	15.5	14.7	14.4	14.2	13.4	13.0	13.7	14.2	14.8	13.9	14.4	13.9
Nd	53.4	54.3	60.5	57.3	56.2	55.6	52.4	52.4	54.3	56.3	58.3	55.8	57.0	53.9
Sm	10.0	10.3	11.6	10.8	11.0	10.6	10.2	10.0	10.4	10.9	11.5	10.8	10.8	10.7
Eu	1.95	2.05	2.35	2.17	2.17	2.15	2.02	1.98	2.14	2.20	2.32	2.19	2.24	2.15
Gd	8.97	9.67	10.3	9.82	9.99	9.40	9.26	9.26	9.39	10.2	10.7	10.4	9.77	9.81
Tb	1.40	1.47	1.58	1.48	1.50	1.45	1.41	1.44	1.45	1.50	1.57	1.55	1.53	1.52
Dy	7.82	8.30	8.52	8.13	8.18	8.08	7.57	7.64	8.00	8.15	8.57	8.57	8.41	8.28
Ho	1.48	1.58	1.67	1.56	1.56	1.57	1.46	1.47	1.57	1.57	1.64	1.62	1.70	1.62
Er	4.43	4.68	4.76	4.57	4.57	4.51	4.32	4.40	4.49	4.56	4.84	4.78	4.74	4.74
Tm	0.72	0.74	0.77	0.72	0.71	0.73	0.69	0.70	0.73	0.74	0.77	0.77	0.77	0.76
Yb	4.60	4.58	5.00	4.69	4.57	4.72	4.44	4.53	4.67	4.72	4.97	4.95	4.96	5.01
Lu	0.76	0.77	0.82	0.76	0.77	0.77	0.72	0.76	0.78	0.79	0.84	0.81	0.82	0.83
Hf	5.65	5.58	5.70	5.46	5.39	5.54	4.98	4.92	5.32	5.30	5.49	5.76	5.53	5.61
Ta	1.21	1.26	1.38	1.18	1.20	1.44	1.19	1.19	1.38	1.22	1.19	1.55	1.39	1.28
Pb	53.6	52.8	64.2	55.6	57.4	55.4	49.7	48.1	48.8	53.1	56.8	57.5	63.3	59.7
Th	28.4	28.0	30.8	28.5	29.4	28.9	26.7	26.3	27.7	29.7	30.4	30.2	30.4	28.3
	BX-35	BX-36	BX-37	BX-38	BX-39	BX-40	BX-41	BX-42	BX-43	BX-44	BX-45	BX-46	BX-47	BX-48
	70	72	74	76	78	80	82	84	86	88	90	92	94	96
	17.29	17.71	18.13	18.38	18.85	19.31	19.78	20.24	20.71	21.18	21.64	22.11	22.57	23.04
Sc	31.4	31.5	31.9	32.6	31.3	31.0	29.9	31.8	32.3	32.5	32.4	31.1	32.3	31.6
V	248	246	257	306	272	283	258	276	281	228	209	209	220	203
Cr	145	156	145	150	159	155	143	149	152	180	156	152	151	150
Co	23.8	23.6	24.5	24.8	24.5	24.2	23.2	23.0	23.4	20.7	18.6	18.6	18.8	16.2
Ni	77.0	73.8	71.2	68.8	69.5	72.8	66.5	66.6	67.7	74.2	59.0	–	56.6	50.3
Cu	204	239	206	163	165	158	144	144	139	97.2	87.1	85.2	83.2	74.0
Zn	96.6	79.4	84.8	–	77.0	81.8	79.6	80.9	82.0	81.7	72.1	72.3	75.9	67.7
Ga	36.4	36.9	36.6	35.6	35.4	36.0	35.9	35.8	36.5	35.9	35.0	34.8	35.5	33.2
Ge	3.65	3.64	3.66	3.60	3.53	3.50	3.34	3.28	3.40	3.26	3.20	3.16	3.16	3.26
Rb	207	201	202	191	188	198	202	203	210	217	212	223	234	233
Sr	95.0	99.8	102	105	99.3	92.2	85.5	89.2	89.6	82.5	79.1	76.2	78.4	74.4
Y	43.7	44.8	45.5	46.0	42.8	42.5	41.2	42.0	43.8	43.0	41.5	43.0	44.4	43.7
Zr	221	210	205	205	202	209	201	213	211	202	208	212	231	225
Nb	18.7	18.4	17.5	17.2	17.8	17.3	17.6	16.8	17.0	17.1	17.0	16.7	17.9	17.5
Ba	651	654	630	619	625	615	610	635	619	622	634	629	661	662
La	56.6	57.2	59.2	61.2	57.3	55.8	54.6	55.6	58.5	58.1	54.9	56.9	59.6	57.3
Ce	136	141	143	149	141	134	133	137	142	142	137	141	143	140
Pr	14.7	15.3	15.3	16.3	15.4	14.5	14.4	14.7	15.3	15.1	14.8	14.8	15.1	14.8
Nd	57.9	61.6	62.4	64.9	62.2	59.4	59.6	60.0	62.2	61.0	59.4	59.3	60.3	57.4
Sm	11.5	11.9	12.1	12.8	12.0	11.6	11.7	11.8	12.2	12.0	11.4	11.3	11.4	10.9
Eu	2.26	2.45	2.45	2.56	2.51	2.36	2.36	2.36	2.43	2.40	2.33	2.26	2.28	2.25
Gd	10.3	10.6	10.9	11.7	10.8	10.5	10.7	10.7	11.0	10.8	10.1	10.4	10.3	9.97
Tb	1.58	1.64	1.66	1.71	1.63	1.57	1.57	1.61	1.63	1.63	1.60	1.60	1.61	1.57
Dy	8.66	8.93	8.96	9.10	8.77	8.45	8.61	8.65	9.03	8.86	8.43	8.63	8.90	8.83
Ho	1.67	1.81	1.72	1.73	1.72	1.67	1.66	1.67	1.72	1.71	1.69	1.66	1.68	1.74
Er	4.85	5.05	5.00	5.11	4.83	4.93	4.82	4.90	5.05	5.07	4.69	4.90	5.08	4.88
Tm	0.78	0.82	0.79	0.81	0.78	0.77	0.75	0.79	0.79	0.79	0.74	0.77	0.78	0.71
Yb	5.19	5.28	5.08	5.19	5.13	4.98	4.93	5.12	5.18	5.02	4.84	5.02	5.04	5.05
Lu	0.84	0.89	0.85	0.87	0.85	0.84	0.83	0.86	0.86	0.83	0.80	0.81	0.85	0.84
Hf	6.11	5.81	5.48	5.60	5.58	5.55	5.64	5.85	5.84	5.65	5.71	5.92	6.17	6.31
Ta	1.34	1.43	1.26	1.28	1.36	1.29	1.31	1.27	1.26	1.29	1.29	1.26	1.37	1.63
Pb	58.6	63.1	58.0	58.5	64.2	67.4	65.6	67.7	69.7	63.7	62.8	62.6	66.6	60.4
Th	27.9	29.0	28.9	29.9	29.7	29.1	28.6	29.5	30.8	31.2	30.4	30.0	30.6	29.9

(*continued on next page*)

Table 2 (*continued*)

	BX-49	BX-50	BX-51	BX-52	BX-53	BX-54	BX-55	BX-56	BX-57	BX-58	BX-59	BX-60	BX-61	BX-62
	98	100	102	104	106	108	110	112	114	116	118	120	122	124
	23.42	23.81	24.19	24.57	24.95	25.34	25.72	26.10	26.48	26.87	27.25	27.63	27.68	27.74
Sc	30.2	30.5	30.3	31.8	31.6	32.2	30.5	30.3	30.4	29.0	28.8	31.3	31.2	30.7
V	197	188	200	214	243	244	229	214	195	189	191	210	241	220
Cr	138	147	142	157	147	155	145	142	149	137	137	158	162	161
Co	15.1	14.8	16.7	16.4	19.0	19.0	17.0	16.8	16.5	15.4	15.2	17.2	20.3	19.6
Ni	44.8	45.9	48.6	–	54.2	53.0	51.2	47.9	47.4	46.8	47.2	53.9	59.9	–
Cu	53.3	64.0	67.2	85.6	100	84.9	70.3	56.2	58.3	71.9	67.5	86.0	77.3	75.3
Zn	73.2	63.6	72.2	67.0	75.2	69.6	72.3	69.4	63.0	71.9	71.9	80.2	97.1	69.0
Ga	34.4	33.4	35.0	34.3	34.3	34.1	33.5	33.6	34.0	33.5	32.1	33.9	33.2	32.3
Ge	3.39	3.30	3.46	3.41	3.37	3.37	3.40	3.35	3.36	3.31	3.30	3.44	3.40	3.42
Rb	250	238	252	241	245	246	254	269	263	257	254	249	253	238
Sr	67.6	71.4	69.9	77.2	74.2	74.9	69.5	64.6	63.3	55.7	56.8	73.2	101	109
Y	44.5	43.4	45.6	44.4	45.0	45.9	44.8	44.6	41.0	39.7	40.1	41.7	47.0	47.5
Zr	228	227	247	206	221	228	223	226	211	223	212	223	205	212
Nb	20.7	17.1	20.8	16.9	17.3	16.9	16.9	17.9	17.6	20.8	18.4	17.1	15.9	16.5
Ba	668	670	665	679	659	691	682	710	716	697	692	720	745	745
La	59.4	57.0	60.6	61.3	61.0	59.9	58.7	58.8	54.6	49.6	50.3	53.5	65.0	64.1
Ce	143	141	148	155	151	151	144	139	131	114	118	132	168	169
Pr	14.8	14.7	15.1	15.8	15.1	15.5	14.8	14.3	13.9	11.9	12.4	14.1	16.9	17.2
Nd	56.9	57.0	58.7	61.8	59.6	60.1	57.4	55.8	53.5	47.5	48.1	54.1	67.4	68.4
Sm	11.0	10.7	11.1	11.6	11.3	11.4	10.9	10.8	10.1	9.0	9.0	10.1	12.8	12.9
Eu	2.11	2.17	2.20	2.36	2.27	2.31	2.14	2.08	1.97	1.75	1.80	2.02	2.57	2.63
Gd	9.94	9.86	10.6	10.3	10.8	10.3	10.1	9.89	9.12	8.28	8.43	9.08	12.0	11.7
Tb	1.56	1.57	1.59	1.63	1.60	1.64	1.62	1.59	1.48	1.34	1.38	1.49	1.77	1.77
Dy	8.85	8.66	8.77	8.94	8.97	8.97	8.80	8.80	8.23	7.68	8.04	8.24	9.50	9.32
Ho	1.73	1.74	1.71	1.76	1.73	1.80	1.68	1.72	1.62	1.52	1.57	1.62	1.81	1.84
Er	4.99	4.82	5.02	4.94	5.13	5.04	5.04	5.08	4.55	4.53	4.63	4.58	5.28	5.33
Tm	0.79	0.79	0.80	0.79	0.80	0.81	0.78	0.78	0.73	0.71	0.71	0.75	0.83	0.87
Yb	5.10	4.97	5.17	5.07	5.13	5.30	5.08	5.10	4.80	4.68	4.65	4.83	5.38	5.55
Lu	0.83	0.83	0.86	0.84	0.85	0.88	0.85	0.86	0.80	0.77	0.78	0.81	0.93	0.96
Hf	6.01	6.21	6.64	5.70	5.94	6.34	6.08	6.27	5.94	6.10	5.91	6.02	5.57	5.59
Ta	1.43	1.26	1.44	1.26	1.43	1.26	1.19	1.46	1.32	1.37	1.37	1.34	1.18	1.20
Pb	61.6	61.6	62.9	63.3	65.8	61.6	56.7	52.4	51.6	55.8	59.6	66.2	65.9	63.9
Th	29.0	29.1	30.3	30.7	31.1	30.5	29.9	29.3	29.7	27.1	28.1	30.3	33.1	32.0
	BX-63	BX-64	BX-65	BX-66	BX-67	BX-68	BX-69	BX-70	BX-71	BX-72	BX-73	BX-74	BX-75	BX-76
	126	128	130	132	134	136	138	140	142	144	146	148	150	152
	27.79	27.84	27.90	27.95	28.00	28.06	28.11	28.16	28.22	28.27	28.32	28.38	28.43	28.48
Sc	30.9	32.4	32.8	32.5	32.5	32.7	31.3	30.8	31.3	30.2	30.9	28.8	28.5	29.8
V	236	260	291	281	281	314	239	236	219	228	209	206	194	172
Cr	156	170	163	173	177	174	160	148	153	144	149	137	134	137
Co	23.0	23.7	28.4	34.4	35.1	51.3	31.0	25.5	23.9	26.5	19.8	18.7	17.5	19.0
Ni	65.4	72.1	83.3	89.6	90.6	130.2	77.1	66.8	63.2	64.0	54.2	47.6	45.9	49.6
Cu	96.6	94.2	95.2	140	129	154	104	83.5	81.8	93.8	67.6	49.3	49.6	52.9
Zn	78.8	69.9	86.3	78.3	81.4	89.0	85.8	78.4	67.1	73.8	67.3	65.6	64.7	57.7
Ga	34.4	34.6	31.4	35.2	36.5	36.7	36.9	34.4	34.9	33.1	33.4	30.4	29.8	31.0
Ge	3.65	3.77	3.42	3.92	4.06	4.53	3.96	3.89	3.75	3.73	3.66	3.46	3.52	3.50
Rb	243	233	212	233	233	223	238	244	243	238	244	221	226	222
Sr	114	123	118	112	107	113	93.3	96.7	96.9	103	107	116	120	118
Y	49.9	49.7	43.9	46.9	44.4	42.9	44.2	46.9	46.4	46.6	50.9	52.3	52.5	51.9
Zr	207	203	209	211	202	198	203	210	199	185	225	201	176	182
Nb	15.8	16.7	14.5	16.3	16.6	16.0	17.2	19.2	17.1	16.3	17.3	16.1	16.4	17.2
Ba	726	740	705	700	698	660	721	722	746	735	785	766	774	792
La	65.0	65.3	58.8	59.6	56.7	57.2	59.3	64.9	64.3	66.3	67.2	73.4	76.5	74.2
Ce	171	174	152	156	147	146	147	158	155	159	160	172	177	171
Pr	17.3	17.8	15.7	16.3	15.6	15.4	15.7	16.7	16.8	17.1	18.0	19.3	19.6	19.8
Nd	69.5	71.8	63.3	65.2	62.2	61.5	62.3	66.7	66.0	67.7	70.4	76.5	78.2	78.3
Sm	13.4	13.9	12.3	12.4	11.9	11.9	12.1	12.8	12.6	13.1	13.1	14.6	14.8	14.6
Eu	2.64	2.80	2.43	2.53	2.44	2.36	2.42	2.53	2.55	2.56	2.74	2.85	2.90	3.02
Gd	12.2	12.3	11.2	11.1	10.7	10.8	10.6	11.5	11.2	11.8	11.9	12.8	13.6	13.0
Tb	1.77	1.78	1.64	1.68	1.58	1.58	1.61	1.77	1.72	1.76	1.77	1.92	1.93	1.93
Dy	9.49	9.49	8.67	9.00	8.46	8.80	8.64	9.30	9.16	9.49	9.76	10.2	10.2	10.1
Ho	1.85	1.90	1.68	1.81	1.69	1.71	1.69	1.78	1.79	1.81	1.91	1.90	1.94	1.95
Er	5.62	5.44	4.99	5.15	4.80	5.10	4.86	5.19	5.05	5.32	5.39	5.73	5.79	5.38
Tm	0.88	0.87	0.78	0.83	0.78	0.80	0.79	0.83	0.79	0.81	0.85	0.88	0.88	0.86
Yb	5.77	5.73	5.14	5.45	5.11	5.17	5.08	5.28	5.06	5.19	5.40	5.61	5.48	5.30
Lu	1.00	0.96	0.87	0.93	0.86	0.88	0.84	0.90	0.83	0.85	0.89	0.94	0.93	0.89
Hf	5.69	5.40	5.07	5.77	5.38	5.57	5.54	5.75	5.50	5.23	5.85	5.66	4.82	4.68
Ta	1.20	1.19	1.11	1.16	1.16	1.17	1.24	1.54	1.26	1.33	1.22	1.25	1.27	1.25
Pb	63.8	62.3	61.6	68.5	69.1	77.5	65.7	61.9	58.7	62.6	60.0	58.7	53.4	47.2
Th	34.5	34.2	31.7	33.1	32.3	34.6	29.8	31.4	29.8	30.3	28.7	29.1	28.5	26.5

Table 2 (*continued*)

	BX-77	BX-78	BX-79	BX-80	BX-81	BX-82	BX-83	BX-84	BX-85	BX-86	BX-87	BX-88	BX-89	BX-90
	154	156	158	160	162	164	166	168	170	172	174	176	178	180
	28.54	28.59	28.64	28.70	28.75	28.96	29.17	29.37	29.58	29.79	30.00	30.20	30.41	30.62
Sc	30.1	28.4	30.9	30.5	29.8	28.2	30.8	29.5	30.1	28.6	29.4	28.5	29.9	28.6
V	178	178	190	190	191	170	207	198	189	188	195	173	193	178
Cr	132	130	140	137	130	128	133	128	132	123	127	127	130	131
Co	17.8	16.9	17.6	15.9	16.7	15.7	19.0	17.1	18.8	18.9	20.8	16.4	13.8	17.8
Ni	49.5	50.0	52.2	49.0	48.2	47.9	58.2	50.2	54.3	49.4	56.9	49.4	44.9	57.7
Cu	59.8	60.5	64.1	64.7	56.3	56.0	94.5	69.6	77.5	64.5	72.2	66.5	58.0	68.6
Zn	67.9	65.7	65.0	71.1	72.8	62.4	78.2	76.6	79.9	96.0	103	80.3	90.0	86.0
Ga	31.8	32.0	33.7	33.0	35.1	35.0	35.4	33.6	34.3	33.4	34.1	33.3	28.6	33.0
Ge	3.44	3.44	3.47	3.36	3.43	3.36	3.64	3.49	3.49	3.49	3.52	3.34	2.92	3.33
Rb	224	226	232	227	244	241	242	241	235	235	238	228	206	227
Sr	97.0	82.8	74.2	71.1	59.6	51.4	60.8	56.8	56.8	51.5	53.6	49.6	52.7	50.9
Y	50.8	48.2	46.9	46.4	42.1	41.5	43.9	42.8	42.7	41.4	42.7	38.9	37.6	38.1
Zr	198	213	214	205	192	242	229	217	235	203	226	212	238	201
Nb	17.4	18.3	18.1	17.8	18.4	18.9	18.2	17.7	18.0	18.0	18.1	18.2	15.9	18.0
Ba	737	712	722	718	719	708	706	705	703	697	714	695	728	692
La	71.1	64.6	61.8	59.1	56.4	47.7	57.2	56.0	53.3	52.0	53.7	49.1	48.7	50.4
Ce	161	146	141	135	124	105	126	123	119	113	118	108	104	112
Pr	18.3	16.4	16.0	15.5	14.3	12.2	14.4	14.0	13.6	12.7	13.5	12.5	11.8	13.0
Nd	72.0	64.9	61.4	59.8	55.6	46.8	56.0	54.4	52.3	50.4	52.6	47.8	46.2	49.0
Sm	13.5	12.5	12.0	11.3	10.7	8.94	10.8	10.6	10.1	9.63	9.90	9.11	9.01	9.41
Eu	2.75	2.49	2.43	2.32	2.12	1.84	2.20	2.04	2.04	1.92	1.98	1.84	1.75	1.92
Gd	12.5	11.6	10.4	10.2	9.87	8.26	9.96	9.63	9.20	8.92	9.15	8.13	7.99	8.34
Tb	1.90	1.74	1.66	1.59	1.53	1.38	1.60	1.54	1.48	1.45	1.46	1.37	1.25	1.34
Dy	10.21	9.63	9.14	8.53	8.49	7.92	8.84	8.63	8.27	8.05	8.20	7.62	7.17	7.47
Ho	1.95	1.84	1.79	1.68	1.62	1.60	1.69	1.66	1.66	1.60	1.61	1.52	1.42	1.48
Er	5.63	5.37	4.99	4.65	4.67	4.57	5.03	4.85	4.61	4.68	4.75	4.27	3.99	4.13
Tm	0.87	0.83	0.79	0.76	0.74	0.73	0.77	0.77	0.76	0.74	0.75	0.70	0.65	0.68
Yb	5.52	5.29	5.01	4.86	4.74	4.65	4.89	4.94	4.89	4.71	4.82	4.41	4.25	4.35
Lu	0.92	0.85	0.82	0.79	0.77	0.77	0.82	0.81	0.78	0.78	0.80	0.71	0.68	0.70
Hf	5.49	5.76	5.67	5.42	5.46	6.66	6.59	6.25	6.33	5.86	6.47	5.93	4.96	5.61
Ta	1.43	1.38	1.30	1.28	1.41	1.39	1.44	1.38	1.35	1.39	1.39	1.37	1.22	1.35
Pb	49.3	47.7	45.3	42.1	46.7	45.1	55.0	52.8	49.8	50.7	54.9	48.5	46.4	50.9
Th	28.9	28.0	27.0	26.6	27.6	24.2	29.0	27.7	26.7	27.5	28.0	26.4	24.7	27.1

ID	BX-91	BX-92	BX-93	BX-94	BX-95	BX-96	BX-97	BX-98	BX-100
Depth (cm)	182	184	186	188	190	192	194	196	200
Age (ka)	30.83	31.03	31.24	31.45	31.66	31.86	32.07	32.28	32.70
Sc	28.3	28.6	27.1	30.8	31.0	30.9	31.6	31.7	32.3
V	186	190	191	209	234	235	228	245	238
Cr	123	125	128	144	140	140	147	143	151
Co	15.2	15.0	21.5	20.6	25.6	30.7	26.3	49.6	49.5
Ni	48.6	54.3	58.7	62.0	61.9	66.3	64.5	90.1	79.4
Cu	63.4	62.5	69.6	90.3	72.0	83.6	79.2	98.8	107
Zn	86.6	90.4	92.8	104	98.8	97.6	96.5	96.5	89.3
Ga	32.4	32.2	34.1	33.8	34.3	33.4	34.3	33.1	34.3
Ge	3.39	3.32	3.48	3.41	3.47	3.38	3.53	3.54	3.53
Rb	227	211	228	219	229	222	224	216	220
Sr	50.7	51.4	50.9	62.6	68.4	72.8	76.2	81.5	76.8
Y	42.1	37.9	47.9	40.9	51.1	53.5	51.6	52.0	51.4
Zr	201	221	210	199	197	206	217	221	205
Nb	17.6	17.1	17.1	17.3	16.6	16.2	17.1	16.8	17.2
Ba	678	681	685	668	681	680	686	676	674
La	55.6	49.8	68.4	58.4	73.3	75.3	71.4	75.5	72.4
Ce	120	112	156	132	165	178	168	178	172
Pr	13.7	12.6	17.4	15.1	18.2	19.6	19.2	19.5	19.1
Nd	52.9	49.2	68.3	58.9	73.6	78.4	75.1	77.1	75.1
Sm	10.3	9.44	13.0	11.4	13.9	14.9	14.2	14.8	14.4
Eu	2.02	1.86	2.60	2.32	2.81	3.08	2.95	3.02	2.96
Gd	9.40	8.36	11.8	9.97	13.0	13.7	12.8	13.5	12.7
Tb	1.47	1.37	1.79	1.53	1.93	2.03	1.88	2.02	1.95
Dy	8.48	7.66	9.65	8.23	10.33	10.92	10.21	10.69	10.26
Ho	1.62	1.52	1.81	1.62	1.97	2.05	2.01	2.01	1.99
Er	4.83	4.43	5.39	4.55	5.67	6.05	5.48	5.88	5.50
Tm	0.75	0.68	0.82	0.73	0.90	0.95	0.88	0.89	0.88
Yb	4.91	4.36	5.33	4.66	5.74	5.99	5.58	5.85	5.58
Lu	0.79	0.71	0.87	0.78	0.92	0.98	0.94	0.94	0.92
Hf	6.37	6.01	5.64	5.59	5.92	6.28	5.85	5.81	5.64
Ta	1.39	1.33	1.33	1.28	1.28	1.24	1.25	1.25	1.23
Pb	52.9	52.6	62.4	60.9	65.0	69.5	65.2	73.0	74.7
Th	28.3	26.2	31.1	29.2	31.4	32.0	30.8	30.9	31.1

Table 3
Summary of the calibrated ^{14}C ages of the peats.

Depth (cm)	Sample type	Conventional age (yr BP)	68% range[a] (cal yr BP)	Calendric age[a] (cal yr BP)
76	Grass root	15360 ± 110	18750–18128	18439 ± 311
96	Grass root	19160 ± 120	23249–22659	22954 ± 295
120	Grass root	23040 ± 360	28122–27067	27595 ± 527
162	Grass root	23770 ± 350	29194–28224	28709 ± 485
196	Grass root	27610 ± 490	32744–31861	32303 ± 441

[a] The calibration was carried out by using the Calpal 2007^{online} software at http://www.calpal-online.de.

The ash samples were digested by an HNO_3 + HF acid mixture, and the solutions were used for both major and trace element measurements. Major elements were measured on a Varian Vista Pro ICP-AES at the State Key Laboratory of Geochemistry in Guangzhou Institute of Geochemistry, Chinese Academy of Sciences, and trace elements were measured on a Perkin–Elmer Elan 6000 ICP-MS at the same laboratory. Analytical details of the major and trace element measurements are described in Li et al. (2002) and Liu et al. (1996), respectively. The precision for the measurement of the major elements was better than 1% (Li et al., 2002), and generally better than 5% (RSD) for the trace elements (Liu et al., 1996). The major and trace elemental results are presented in Tables 1 and Table 2, respectively. Several USGS and Chinese soil and sediment standard references, such as GSS-5, GSS-7, GXR-6 (soils), and GSD-9, GSD-12 (sediments) were repeatedly measured with the samples to monitor the quality of the major and trace element measurements, and the results were generally within the range of ±10% (RSD) of the certified values.

The contents of the total organic carbon (TOC) of the samples were measured using a Vario EL III elemental analyzer by Lu (2003), and the results are included in Table 1. Grass roots from five samples were selected for AMS ^{14}C dating (Lu, 2003), and the ages were calibrated using Calpal-2007 online software (Danzeglocke et al., 2010). The calibrated ages are summarized in Table 3.

3. Results

The LOIs at 900 °C vary from 20% to 80%, which are roughly double the TOC contents. An excellent linear correlation exists between the LOIs and TOC contents (Fig. 2), with a correlation coefficient of about 0.97 ($N = 80$, $p < 0.0000001$), and a regression equation of LOI (%) = 1.43 × TOC (%) + 13.9.

Among the major elements, Al_2O_3, MgO, and TiO_2 show limited variation, ranging from 22.42% to 28.82%, from 1.09% to 1.70%, and from 0.79% to 1.08%, respectively. Their averages are 25.95 ± 1.31%, 1.34 ± 0.13%, and 0.92 ± 0.07% (all 1σ), respectively, and the relative deviations are from 5% to 10%. The variations for FeO(T), K_2O, and Na_2O are slightly larger, with averages of 5.36 ± 1.06%, 2.87 ± 0.44%, and 0.20 ± 0.05%, respectively, and relative deviations from 15% to 23%. Large variations are found for CaO, MnO, and P_2O_5, with averages of 2.61 ± 1.04%, 0.03 ± 0.01%, and 0.24 ± 0.11%, respectively, and relative deviations of 40%, 32%, and 47%, respectively.

Most of the trace elements show limited variation, except for some transition metals, such as V, Co, Ni, Cu, Zn, and Sr, which show a relative variation range of >15%. The variation ranges for rare earth elements (From La to Tb), Pb and U are slightly less than the above transition metals, from 10% to 15%. The relative variations of the other elements are generally less than 10%.

4. Discussion

The age model for the peat core in this study is built on five AMS ^{14}C dating results. Linear accumulation rates were assumed between these five age control points to calculate the age of each sample. The top measured sample, at 42 cm, has an age of 11.42 kyr Cal BP, while the bottom sample (200 cm) has an age of 32.70 kyr Cal BP. Thus, the geochemical records of this core extend from the late MIS 3 to the early Holocene, and may provide details of the climatic and environmental changes during the last glacial maximum in this region.

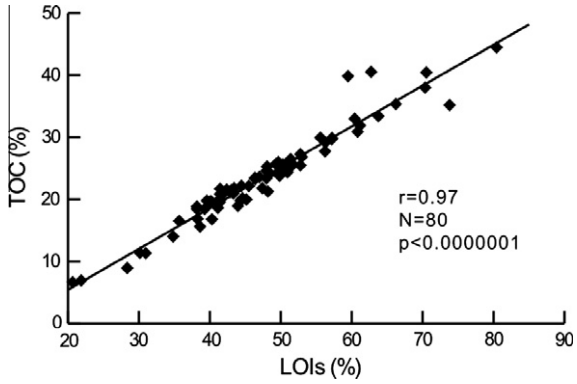

Fig. 2. Correlation between the loss on ignition (LOI) at 900 °C and the TOC content.

4.1. Authigenic contributions of the elements in the peats

The major elements found in the ashes (see Table 1) are typical of silicate dominated sediments. This agrees well with our rough estimates of the mineralogical composition of the ashes using X-ray diffraction (XRD). Rock-forming minerals such as quartz, K-feldspar and albite, as well as clay minerals, account for over 90% of the content of the ashes. Thus silicate weathering products comprise the main part of the inorganic materials of the peats. However, organic materials are the main components of the whole peats/sediments, as indicated by the 20–80% LOIs in Table 1.

The TOC content is certainly the best indicator of organic materials, whereas the LOIs represent all the volatile components. The excellent correlation between the TOC contents and LOIs suggests that organic materials account for most of the LOIs; the ~14% intercept may indicate the presence of non-organic volatile materials, such as water in clays and CO_2 in carbonate. Ti can be one of the best indicators for silicate detritus in sediments (Schroeder et al., 1997; Wei et al., 2004), as Ti generally does not concentrate in biogenic materials and is relatively conserved during weathering, transportation, and deposition processes. Fig. 3 shows the variations in the TOC contents, the LOIs and the Ti concentrations in the peats, where Ti concentrations in the peats are calculated from those in the ashes using the following equation: $[Ti]_{peat} = [Ti]_{ash} \times (100 - LOI)/100$. Inverse variations are clearly shown between the Ti concentrations and the TOC and LOI contents, with high Ti concentrations generally corresponding to low TOC and LOI contents, and vice versa. Robust negative correlations can also be observed between Ti concentrations and the TOC contents and the LOIs, with correlation coefficients of −0.92 ($N = 80$, $p < 0.0000001$) and −0.96 ($N = 80$, $p < 0.0000001$), respectively.

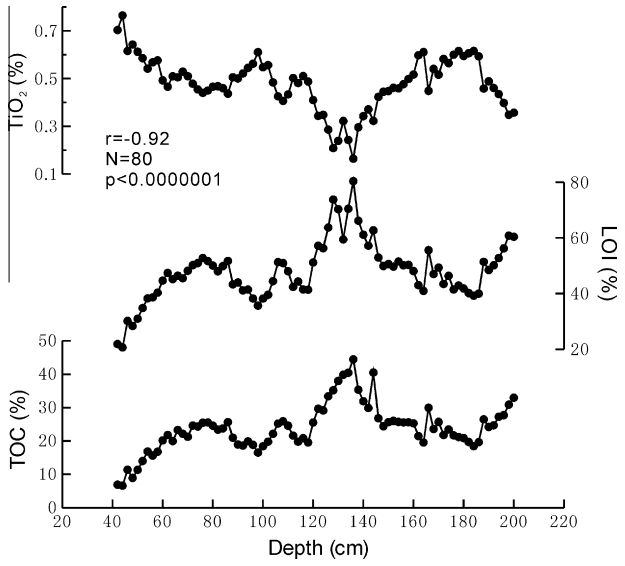

Fig. 3. In-depth variations of the LOIs, the TOC contents, and the TiO_2 contents in the peats. The data demonstrate the correlation between the TiO_2 contents and the LOIs.

The inter-influences of the contents of organic materials and silicate materials in the peats indicated by these co-variations and correlations is called the dilution effect.

After being baked at 900 °C, all the organic materials and other volatile components were removed, but the non-volatile components were retained, along with the elements they contributed. The simplest way to assess such contributions is to test the correlation between the concentration of the elements in the ashes and the TOC contents in the whole peats. As all of the non-volatile components in the organic materials are retained in the ashes, if an element originated in the organic material, its concentration in the ashes will positively correlate with the TOC contents in the peats, and the variation patterns between samples for such elements will be similar to that of the TOC contents. If the elements are not derived from the organic material, there should be no significant positive correlation with the TOC and there may even be a negative correlation. The correlation coefficients between the concentrations of the elements in the ash and the TOC contents in the peats are summarized in Table 4. A significant threshold of $p < 0.001$ is used, and all the positive correlations with correlation significance better than $p < 0.001$ are shown in bold font in Table 4.

The relationships between the element concentrations in the ash and the TOC contents in the peats are clearer when the core is separated into two sections. The top section consists of the samples above 122 cm. The TOC contents in this section are generally less than 25%, with an average of 19.8%. The bottom section consists of the samples below 122 cm. The TOC contents in this section are higher than in the top section, with an average of 27.9%. As shown in Table 4, a number of elements, such as Fe, Mg, Mn, P, V, Co, Ni, Sr, Y, and all the REEs, except for La, Pb, and Th, show significant positive correlations ($p < 0.001$) with the TOC contents of all the samples. Among these elements, P and V show the most robust positive correlations, not only for the whole core, but also for each section. Moreover, the variation patterns of P and V are exactly the same as that of the TOC contents; all the peaks can be correlated with each other (Fig. 4). P is an essential nutrient that can be used by all organisms for energy transport and growth, and it tends to concentrate in biogenic materials such as plants. Its robust and positive correlation with the TOC content, as well as its similar pattern variations, indicate that the P in these peat samples is primarily from organic materials. Similarly, the V in these peat samples may also be mainly from organic materials.

It is worth noting that the Pb in the peats is closely associated with organic materials; the correlation coefficient between Pb and the TOC contents is above the $p < 0.001$ threshold throughout the whole core and in both sections (Table 4). This is consistent with the observation that plants can generally accumulate Pb from soils and dust, resulting in fairy high Pb concentrations in roots and leaves (Singh et al., 1997). Fig. 5 shows the down-core variation of the Pb/Ti ratios. The Pb/Ti ratios range from 7×10^{-3} to 15.4×10^{-3}, which are significantly higher than the average upper continental crust ratio of about 4.43×10^{-3} (Rudnick and Gao, 2003). It will be shown in the following section that the provenance of the silicate materials has not changed significantly in this

Table 4
Correlations between the concentrations of the elements and TOC.

Element	Total ($N = 80$)	>122 cm ($N = 40$)	<122 cm ($N = 40$)	Element	Total ($N = 80$)	>122 cm ($N = 40$)	<122 cm ($N = 40$)
Al_2O_3	0.03	−0.43	**0.59**	Zr	−0.20	0.05	−0.27
CaO	0.20	0.14	**0.77**	Nb	−0.31	−0.01	−0.48
Fe_2O_3(T)	**0.36**	−0.27	**0.82**	Ba	0.23	−0.52	−0.01
K_2O	−0.21	−0.19	−0.68	La	0.33	0.07	0.19
MgO	**0.59**	0.26	**0.83**	Ce	**0.43**	0.19	0.46
MnO	**0.40**	−0.21	**0.74**	Pr	**0.45**	0.34	0.31
Na_2O	0.25	0.44	**0.90**	Nd	**0.48**	0.44	0.35
P_2O_5	**0.59**	**0.71**	**0.90**	Sm	**0.49**	**0.48**	0.38
TiO_2	−0.36	−0.06	−0.77	Eu	**0.49**	**0.49**	0.36
				Gd	**0.47**	**0.51**	0.35
Sc	0.24	0.11	**0.79**	Tb	**0.46**	**0.59**	0.27
V	**0.53**	**0.62**	**0.86**	Dy	**0.43**	**0.58**	0.21
Cr	0.34	0.11	**0.86**	Ho	**0.50**	**0.62**	0.27
Co	**0.47**	−0.11	**0.67**	Er	**0.47**	**0.63**	0.28
Ni	**0.46**	0.13	**0.80**	Tm	**0.51**	**0.61**	0.33
Cu	0.19	0.39	**0.85**	Yb	**0.53**	**0.70**	0.39
Zn	−0.15	−0.36	−0.03	Lu	**0.57**	**0.73**	0.47
Ga	−0.17	−0.27	0.43	Hf	−0.11	0.27	−0.33
Ge	0.27	−0.31	**0.79**	Ta	−0.25	0.15	−0.54
Rb	0.03	−0.19	0.12	Pb	**0.43**	**0.48**	**0.64**
Sr	**0.42**	0.22	**0.71**	Th	**0.52**	0.36	**0.72**
Y	**0.39**	0.30	0.23	U	−0.21	−0.24	−0.10

* The data shown in bold style indicate that they are above the significance thresholds of the correlations as follows: $N = 80$, $r = 0.35$, $p < 0.001$; and $N = 40$, $r = 0.48$, $p < 0.001$.

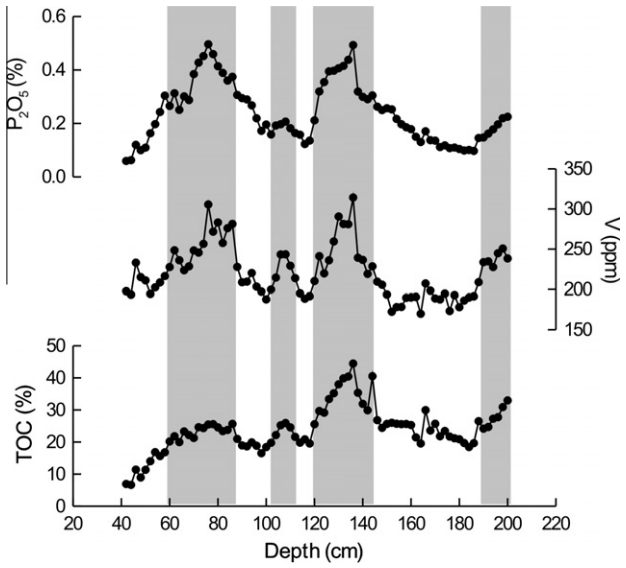

Fig. 4. In-depth variations of the TOC contents of the peats and the P_2O_5 and V concentrations in the ashes. The shaded bars mark the in-pace variations of these records.

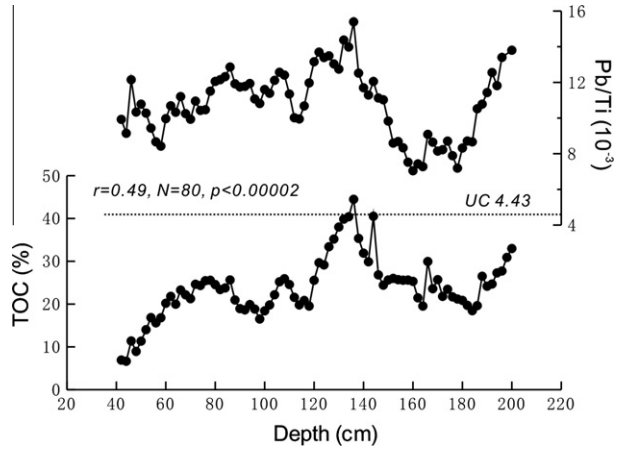

Fig. 5. In-depth variations of the Pb/Ti ratios in the ashes and the TOC contents of the peats. The horizontal dash line marks the average Pb/Ti ratio of the upper crust. The data demonstrate the correlation between the Pb/Ti ratios and the TOC contents.

core. Thus, heterogenic Pb concentrations in the silicates are not the likely cause of such large Pb/Ti variations, and much of the Pb in these peats may come from non-silicate materials. This is further supported by the similar variation patterns of the Pb/Ti ratios and the TOC contents (Fig. 5). There is a significant positive correlation between the Pb/Ti ratios and the TOC contents, with a correlation coefficient of 0.49 ($N = 80$, $p < 0.00002$). Furthermore, in the section below 120 cm, which has higher TOC values, the correlation is much more significant ($r = 0.75$, $N = 40$, $p < 0.0000001$). It is thus likely that the Pb in peats is largely from organic materials. Pb is among the most concerned elements in peats, and both Pb concentrations and isotopes have been broadly used in tracing anthropogenic impacts on the environment, in particular atmospheric inputs by anthropogenic activities (Farmer et al., 2006; Kamenov et al., 2009; Shotyk et al., 2001). The likely enrichment of Pb by organic materials, shown in our analysis, suggests on the one hand, that Pb in peats and organic rich sediments is indeed sensitive to changes in environmental Pb due to the accumulation ability of plants. On the other hand, plants may accumulate such Pb enrichment through soils rather than through the absorption of atmospheric dust. Therefore, caution is appropriate when using Pb in peats to trace atmospheric inputs, in particular in peat pots where water flow influence is significant or Pb recycling is active.

The apparent positive correlations between REEs (except for La) can only be observed in the top section of the core (Table 4), whereas correlations in the bottom section of the core are poor. The relative deviations in the variation in the REE concentrations in the top section are generally less than 10%, close to the analytical precision for REEs, which suggests that the apparent correlations to TOC contents in the top section may not be meaningful. However, in the bottom section, even though the variations in the REE concentrations are slightly larger and the TOC contents are much higher, correlations between them are all below the $p < 0.001$ significance level. Thus, the correlations between the REEs and the TOC contents are not valid, and the amount of REEs in these peats that come from organic materials may be very small.

In addition to P, V, and Pb, some other elements also show significant and positive correlations with the TOC contents in the bottom section of the core (Table 4). These elements include most of the major elements, except for K and Ti, and most of the transition metals, such as Sc, Cr, Co, Ni, Cu, Sr, and Th. The significant positive correlation of these elements with the TOC contents indicates that they may also be partly derived from the organic materials.

In addition to organic materials, carbonates are the other important non-silicate component of peats. As carbonates are generally rich in Ca, Mg, and Sr, the existence of carbonates may result in robust positive correlations between the concentrations of each two of these elements. An alternative method to determine the existence of carbonate in sediments is to show their Ti normalized ratios (Schroeder et al., 1997; Wei et al., 2004). As Ti mainly concentrates in silicate components, and its concentration in carbonates is very low, if carbonates exist the Ti normalized ratios for Ca, Mg and Sr should be significantly higher than their corresponding values in the silicate components. Fig. 6 shows the down-core variations of the CaO/TiO_2, MgO/TiO_2, Sr/Ti, $FeO(T)/TiO_2$ and MnO/TiO_2 ratios. They all show a similar variation pattern, and there are robust correlations between each pair of these elements; the correlation efficient is generally >0.80 ($N = 80$, $p < 0.0000001$). Moreover, these Ti normalized ratios all show large variation amplitudes, with relative variations up to 200–300% (Fig. 6). These indicate that Ca, Mg, Sr, Fe and Mn are closely associated with carbonates in these peats. Higher Ti normalized ratios for these elements in the core, shade-marked in Fig. 6, indicate higher carbonate contents. These sections also generally have higher TOC contents.

The close association of Fe and Mn with carbonates in these peats is interesting. Fe and Mn concentrations in normal carbonates, such as biogenic carbonates and those chemically deposited under oxic environments, are generally very low; there is no positive correlation between Fe and Mn concentrations and carbonate contents. However, authigenic $FeCO_3$ and $MnCO_3$ can be formed in anoxic sediments where Fe^{2+} and Mn^{2+} supplies are sufficient (Calvert and Pedersen, 1996; Pedersen and Price, 1982; Postma, 1981, 1982). The close correlations between Fe, Mn, and Ca suggest this may be the case in these sediments. Moreover, the higher Fe and Mn concentrations are generally accompanied by higher TOC contents as shown in Fig. 6. This agrees with the fact that organic materials are the most effective reductant in sediments. More organic materials in sediments may consume more oxidants and result in more reductive conditions, which may favor the deposit of authigenic $FeCO_3$ and $MnCO_3$. As a result, it is likely that the Fe and Mn in these peats are largely from authigenic carbonates.

K, Ti, Zn, Ge, Rb, Zr, Nb, Ba, La, Hf, Ta, and U concentrations in the ashes show no positive correlations with the TOC contents; some even show negative correlations, both in the separated sec-

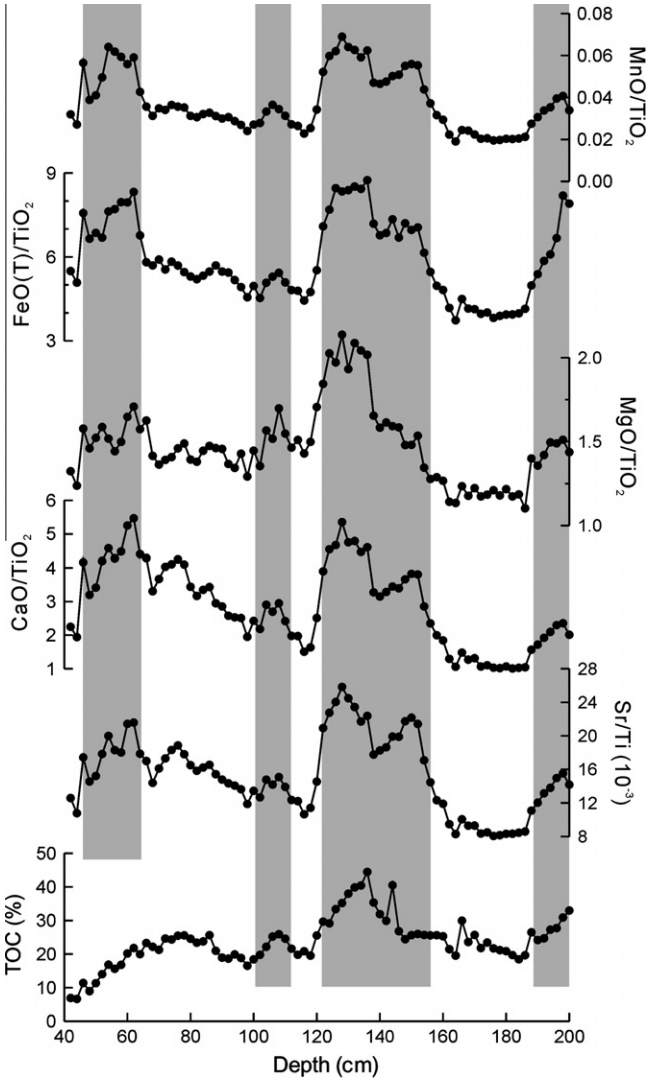

Fig. 6. In-depth variations of CaO/TiO_2, MgO/TiO_2, Sr/Ti, FeO (T)/TiO_2, and MnO/TiO_2 and the TOC contents in the peats. Shaded bars mark the in-pace variations of these records.

tions and in the entire core. These elements probably did not originate in the organic materials or other authigenic components, but are mainly hosted in the silicate detrital components of the peats.

4.2. Provenance of the silicate materials

As previously mentioned, silicate materials are the main components of the ashes. These materials may have been incorporated into the peat through local weathering products, such as soils and sediments in the local drainage. However, dust from north China, particularly from the Loess Plateau, may also contribute to the peats, as these peats were deposited during the last glacial maximum, when both the drought in north China and the strength of the winter monsoon were enhanced (Wang et al., 2008). This would have resulted in enhanced dust fluxes to the south of the Plateau.

Elements such as Sc, Ti, Zr, Hf, Nb, Ta, REE, and Th are generally conserved during chemical weathering (Braun et al., 1993; Nesbitt and Markovics, 1997), and the discrimination diagrams of these elements can generally be used to trace the origins of the silicate materials (Bhatia and Crook, 1986; Fralick and Kronberg, 1997). The above analysis suggests that the Sc and Th in the peat samples from the bottom section of the core were partly derived from organic materials (Table 4). Thus, we exclude Sc and Th from the provenance tracing.

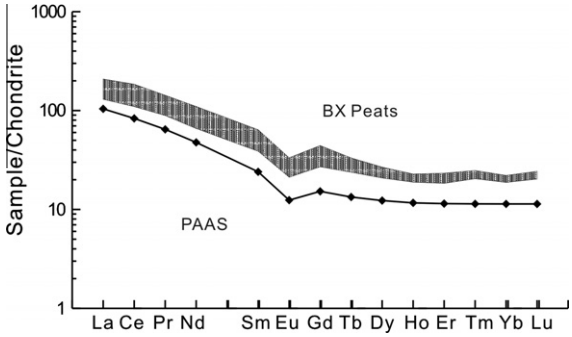

Fig. 7. Range of the chondrite-normalized REE patterns of the peat ashes. The pattern for PAAS is also presented for comparison.

The REEs in these peats do not come from organic materials, and they can be used in provenance tracing. Fig. 7 shows the chondrite normalized REE patterns of the peat samples, as well as those of the Post-Archaean average Australian sedimentary rock (PAAS). All the peat samples exhibit nearly the same REE patterns as the PAAS. Additionally, the REE variation ranges of these samples are concentrated in a very narrow range (Fig. 7), suggesting similar sources for the silicate materials in these peats. This can also be inferred from their Eu anomalies, defined as $Eu^* = 2Eu_N/(Sm_N + Gd_N)$, where N indicates normalization by chondrite. The Eu^* varies from 0.61 to 0.66, with an average of 0.633 ± 0.014 (1σ). This value is very close to that of the PAAS, about 0.632 (McLennan, 1989), and the average of some selected loess samples (0.631 ± 0.014) from Xining, Xifeng, and Jixian, which are located at the west, center, and east of the Loess Plateau, respectively (Jahn et al., 2001).

Further provenance information can be obtained from the $TiO_2 * 10/Nb$–La discrimination diagram. Ti, Nb, and La do not come from organic materials, and thus they may provide reliable provenance information (Fig. 8). The loess samples of Jahn et al. (2001) are also plotted in this diagram for comparison. The peat samples are shown in the separated sections mentioned above (Fig. 8). The samples of the two sections largely overlap, and they all concentrate within a narrow range. This again indicates that the silicate materials in these peats are from the same sources. The loess samples also have lower La concentrations and slightly higher $TiO_2 * 10/Nb$ ratios; except for one sample in the diagram, they can be clearly separated from the peats, which implies that the sources of the silicate materials in these peats are different from those of the loess. Giving that dust inputs might be enhanced during the glacial maximum, if dust had contributed to the silicate materials in these peats, it might be from primarily local sources similar to those transported by water flow rather than blown from northern China. Thus, local weathering products may be the main source of the silicate materials in these peats.

4.3. Proxies indicating local chemical weathering intensity

Chemical weathering can alter the mineral and chemical components of continental surfaces, and its products include soils and sediments. Chemical and mineral components in soils and sediments are records of the intensity of chemical weathering in their source regions (Kronberg et al., 1986; Nesbitt and Young, 1982; Wei et al., 2004, 2006).

Ratios between alkali elements, such as K_2O/Na_2O, K/Rb, or Al_2O_3/TiO_2, are good markers of changes in intensity between incipient to moderate weathering (Nesbitt and Markovics, 1997; Nesbitt et al., 1980; Wei et al., 2004). The down-core variations of these ratios are shown in Fig. 9. All these ratios show similar var-

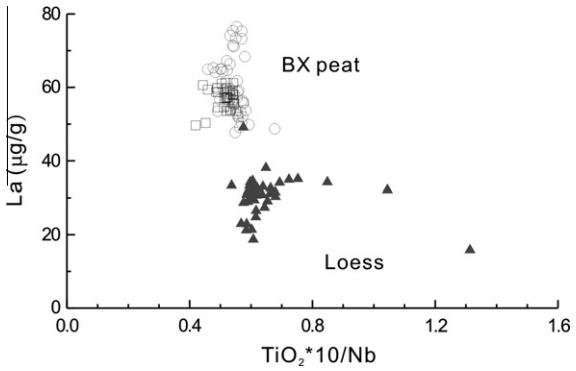

Fig. 8. La–Ti/Nb * 1000 diagrams for the peat ashes and selected loess samples from northern China. Open rectangles indicate the ashes from the top section of the core (above 122 cm), and the open circles indicate those from the bottom section of the core (beneath 122 cm). The solid triangles indicate the loess. The loess data are from Jahn et al. (2001). Except for one loess sample, the ashes and the loess are well-separated.

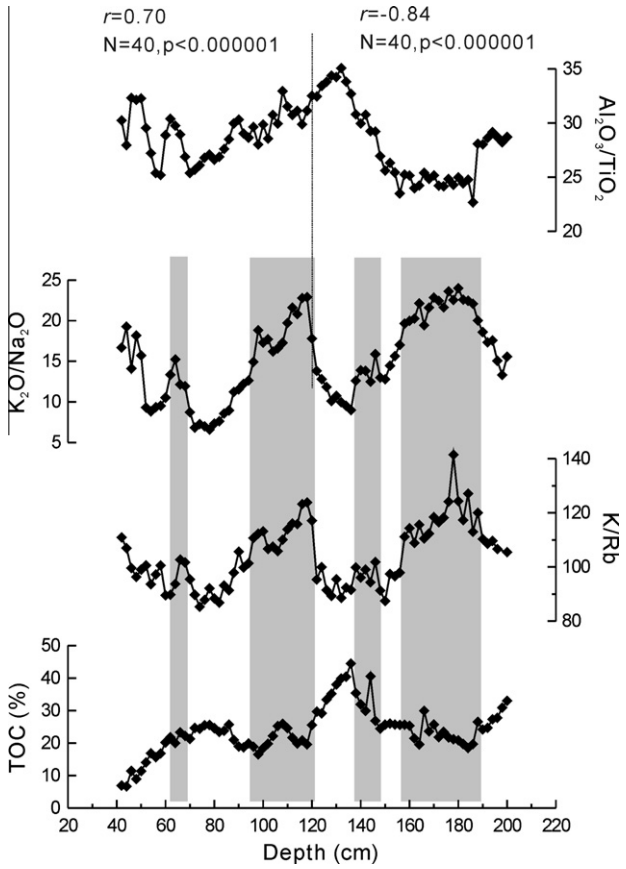

Fig. 9. In-depth variations of the Al_2O_3/TiO_2, K_2O/Na_2O, K/Rb ratios and the TOC contents in the peats. Shaded bars mark the in-pace variations of these records. The data indicate the correlations between Al_2O_3/TiO_2 and K_2O/Na_2O in different sections of the core.

iation patterns in the top section of the core (above 122 cm). This is consistent with the general behaviors of these elements during chemical weathering (Nesbitt and Markovics, 1997; Nesbitt et al., 1980), suggesting that they can reliably indicate the changes in chemical weathering intensity in this basin. Positive correlations can be observed between every pair of ratios in this section. For example, the correlation coefficient between Al_2O_3/TiO_2 and K_2O/Na_2O was 0.70 ($N = 40$, $p < 0.000001$). However, in the bottom section (below 122 cm), Al_2O_3/TiO_2 expressed a variation pattern opposite to the others. A robust and negative correlation occurred between Al_2O_3/TiO_2 and K_2O/Na_2O, with a correlation coefficient of −0.84 ($N = 40$, $p < 0.000001$). As mentioned above, organic materials were the source for some of the Al and Na in this section, whereas Ti and K had no organic origins. Thus, the Al_2O_3/TiO_2 ratios might be expected to increase and K_2O/Na_2O ratios to decrease along with increasing TOC contents, resulting in an inverse variation pattern (Fig. 9). Therefore, using the Al_2O_3/TiO_2 and K_2O/Na_2O ratios in the bottom section of the core may bias the measurement of changes in chemical weathering intensity. .

Unlike the Al_2O_3/TiO_2 and K_2O/Na_2O ratios, as both K and Rb do not originate from non-silicate materials, the ratios of K/Rb can reliably indicate changes in chemical weathering intensity throughout the entire core. As shown in Fig. 9, high K/Rb ratios occur from 96 cm to 122 cm and from 156 cm to 190 cm, indicating stronger chemical weathering intensity, whereas weathering intensities around 80 cm and 130 cm are relatively incipient. It is interesting to see that the K_2O/Na_2O ratios show the same variation pattern as the K/Rb ratios throughout the core even though some Na in the bottom section may be part of the organic contribution. The extra Na from organic materials does not appear to affect the changes in the K_2O/Na_2O ratio caused by chemical weathering in the bottom section. Thus, the K_2O/Na_2O ratios can also be used to measure changes in chemical weathering intensity in these peats.

The variations in chemical weathering intensity shown in Fig. 9 is converse to that of the TOC contents, with high K/Rb and K_2O/Na_2O ratios generally corresponding to low TOC contents. As the TOC contents in peats are controlled by the balance of silicate material inputs and organic material accumulations, intensive chemical weathering, which favors the erosion of continental crust, may enhance the inputs of silicate materials. As a result, the proportion of silicate materials to organic materials increases, and the TOC content decreases. This is how we interpret the inverse variation patterns between chemical weathering intensity and the TOC content.

4.4. Response to the East Asian monsoon climate

Continental chemical weathering is largely controlled by climate. Warm and humid climates favor intensive chemical weathering, and humidity is particularly important (Berner and Berner, 1997). In East Asia, the climate is dominated by the East Asian monsoon, and precipitation in this region is mostly supplied by the East Asian summer monsoon (Ding, 1994). Thus, temporal changes in chemical weathering intensity induced by the change in humidity may closely relate to changes in intensity of the summer monsoon. Evaluating the elemental compositions of our peats may allow us to observe such chemical weathering changes in terrestrial sediments.

Fig. 10 shows the temporal variation of chemical weathering intensity in Baoxiu Basin as represented by the K/Rb and K_2O/Na_2O ratios of these peat samples. The temporal variation in the East Asian summer monsoon, represented by the $\delta^{18}O$ of some stalagmites from Dongge and Hulu caves (Wang et al., 2008), is also shown in Fig. 10 for comparison. Studies by Wang et al. (2008) indicate that the variations in the $\delta^{18}O$ in stalagmites from these two caves are highly consistent, suggesting that they are all controlled by the East Asian summer monsoon (Wang et al., 2008). The more recent $\delta^{18}O$ of the stalagmites from the Wulu and Dashibao caves, which are located to the west of the EASM boundary, very close to Baoxiu Basin (Fig. 1), show similar patterns to those from the Hulu and Dongge caves not only temporally, but also in shape and amplitude (Zhao et al., 2010). This again indicates that the climate changes in this region are largely controlled by the East

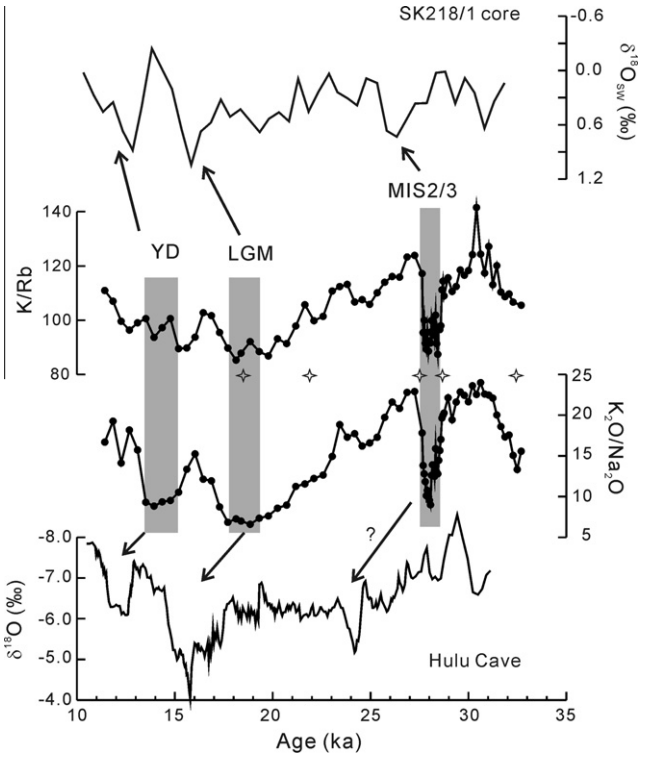

Fig. 10. Comparisons between the variations of the K/Rb and K_2O/Na_2O in the peat ashes, the $\delta^{18}O$ of the stalagmite from the Dongge and Hulu Caves, and the $\delta^{18}O_{SW}$ of core SK218/1 from Bengal Bay. The thin arrows indicate the possible correspondence between these records. YD: Younger Dryas, LGM: Last Glacial Maximum, and MIS 2/3: boundary between Stage 3 and Stage 2. The stars mark the age controls of the peats.

Asian summer monsoon. The variation patterns in the K/Rb and K_2O/Na_2O ratios in the peat are similar to the patterns in the stalagmite $\delta^{18}O$, with higher K/Rb values generally corresponding to lower $\delta^{18}O$ in stalagmites, and vice versa, indicating that the variations of local chemical weathering are active responses to the East Asian summer monsoon changes.

However, time offsets between the corresponding peaks and valleys of the elemental and $\delta^{18}O$ records are generally observed, with the variations of peat K/Rb and K_2O/Na_2O generally leading those of the stalagmite $\delta^{18}O$ by about 3–4 ka. For example, the minimum K/Rb around 18.9 ka may correspond to the highest $\delta^{18}O$ around 15.8 ka with a gap of 3 ka, and the low peat K/Rb ratios around 28 ka may correspond to the high stalagmite $\delta^{18}O$ around 24 ka, a time offset of about 4 ka. The maximum K/Rb value around 30.6 ka may correspond to the minimum $\delta^{18}O$ around 29.4 ka, and the time offset is still about 1 ka.

Time offsets of major climate events between different records from different archives are common in paleoclimate studies. Differences in age models and different responses of the proxies to climatic/environmental changes may account for most of the time offsets. The age model of the peat samples was established from five AMS ^{14}C ages of grass roots. The age control points are shown in Fig. 10. The age models for the stalagmites were based on a number of ^{238}U–^{234}U–^{230}Th ages. Grass roots are good materials for AMS ^{14}C dating, and their calibrated ages could not be biased significantly. However, the number of age control points is very limited compared to those for the stalagmites. Poor age controls in the peat core may partly account for the time offsets between the peat record and the stalagmite record, in particular for the YD and LGM events occurring after 20 ka. The low K/Rb and K_2O/Na_2O ratios between 120 cm and 160 cm were well defined by the two AMS ^{14}C ages (Table 3), yielding ages from 27.6 to 28.7 cal kyr B.P. If this decrease in chemical weathering intensity correlated to the rapid decrease of the EASM strength during 28–29 ka, there is nearly no time offset between these two records. However, the most significant decrease of the EASM strength around this period occurred at the boundary of MIS2/3 as shown in the stalagmite $\delta^{18}O$ record. There is no oscillation as large as those from 27.6 ka to 28.7 ka that can be correlated to the MIS2/3 event in the K/Rb and K_2O/Na_2O records. Thus, we would like to assign the low elemental ratios to MIS2/3 rather than to the rapid decrease of the EASM strength during 28–29 ka recorded by the stalagmite $\delta^{18}O$. This, however, is a very rough estimate. More age controls are needed to establish a better comparison between the chemical weathering records in peats and the EASM changes.

Despite such time offsets, the variations of the peat K/Rb and K_2O/Na_2O ratios and the stalagmite $\delta^{18}O$ are consistent. Lower stalagmite $\delta^{18}O$ indicates more precipitation by the enhanced summer monsoon (Wang et al., 2008). Such correspondence between the peat K/Rb and K_2O/Na_2O ratio and stalagmite $\delta^{18}O$ agrees with the fact that enhanced summer monsoons bring about more precipitation and improve humidity, which favors intensive chemical weathering and results in higher K/Rb and K_2O/Na_2O ratios. Declining summer monsoons result in less precipitation and low humidity, thus decreasing local chemical weathering intensity and resulting in lower K/Rb and K_2O/Na_2O ratios in the peat samples, as during the YD, LGM and MIS2/3 events shown in Fig. 10. Therefore, selected element ratios in the peat samples, such as K/Rb, K_2O/Na_2O and others, actively respond to changes in the East Asian summer monsoon and can proxy changes in local chemical weathering intensity.

Baoxiu Basin is located at the edge of the region influenced by the modern East Asian summer monsoon, as shown in Fig. 1. The consistency between the variation in K/Rb ratios in the peats from Baoxiu and the $\delta^{18}O$ in the stalagmites from the Hulu, Dongge, Wulu and Dashibao caves suggests that the influence of the EASM could also have extended to this region during the last glacial maximum, when the strength of the EASM was significantly decreased. Lower K/Rb and K_2O/Na_2O ratios during the YD and LGM indicate a relative dry climate in this region, which was induced by declined EASM during the LGM.

An alternative interpretation for these chemical weathering records is that they may be responses to changes in the Indian summer monsoon (ISM) during this period, as Baoxiu Basin is next to the region influenced by the ISM at present (Fig. 1). The $\delta^{18}O_{SW}$ of a sediment core, SK218/1, from the Bengal Bay was included in Fig. 10 to illustrate the changes in the ISM (Govil and Naidu, 2011). $\delta^{18}O_{SW}$ shows changes in seawater $\delta^{18}O$, which were calculated from paired Mg/Ca (proxy of SST) and $\delta^{18}O$ of planktonic foraminifer, *G. ruber*. The $\delta^{18}O_{SW}$ variation in core SK218/1 is associated with the terrestrial runoff controlled by changes in summer precipitation, and reflects changes in the ISM (Govil and Naidu, 2011). This record, however, has poor time resolution compared to the stalagmite $\delta^{18}O$, and its variation details could not be identified clearly. The variations in K/Rb and K_2O/Na_2O identified in the peat samples are more like the stalagmite $\delta^{18}O$ than the $\delta^{18}O_{SW}$ of core SK218/1. It is therefore more likely that the changes in chemical weathering intensity in Baoxiu Basin during the last glacial periods were a response to changes in the East Asian summer monsoon. The influence of the ISM does not appear to be an important factor in this region.

5. Summary

The elemental geochemistry of the peats from a peat core collected in Baoxiu Basin, Yunan Province, southwestern China, were used to investigate the extent to which organic materials contrib-

uted to the elemental composition of the peats, and whether change in the elemental composition of the peats could be related to climate change. The main findings are summarized as follows.

(1) Organic materials are the main components of the peats, with TOC contents ranging from 6.64% to 44.46%, and LOIs from 20.63% to 80.43%. Organic materials appear to have made significant contributions to the elements retained in the ashes baked from the peats at 900 °C. Among these elements, P and V appear to be almost entirely from the organic materials with variation patterns very similar to that of the TOC. Al, Na, and most of the transition metals, such as Sc, Cr, Co, Ni, and Cu, as well as Pb and Th are partly from organic materials, particularly in the section below 122 cm. The concentrations of Ca, Mg, Sr, Fe, and Mn in the peats share the same variation pattern, suggesting that they are primarily associated with carbonates, such as authigenic $FeCO_3$ and $MnCO_3$ formed under the anoxic environment of peats. In contrast, K, Ti, Zn, Ge, Rb, Zr, Nb, Ba, REEs, Hf, Ta, and U do not appear to be part of the organic and authigenic materials, and are mainly hosted in the silicate detrital components of the peats.
(2) The silicate materials in the peats are mainly composed of local weathering products. Dust from northern China contributed very little to these peats.
(3) The ratios of K/Rb and K_2O/Na_2O in these peats reliably reflect changes in chemical weathering intensity. Their variation patterns match that of changes in the East Asian summer monsoon from ~30 to ~10 ka, with stronger summer monsoons favoring intense chemical weathering. This suggests that the selected elemental ratios in peats are reliable proxies for changes in the monsoon climate.

Acknowledgements

The authors are most grateful to Xiangling Tu from the Guangzhou Institute of Geochemistry, CAS for his assistance in the ICP-MS measurements. We also thank the two anonymous reviewers for their critical and constructive comments that helped to improve the manuscript. This study was supported by the Knowledge Innovation Project of the Chinese Academy of Sciences (Grant No. KZCX2-YW-138), and the National Natural Sciences Foundation of China (Grant Nos. 40973008, 40272058 and 40830852) This is contribution No. IS-1530 from GIG-CAS.

References

Berner, R.A., Berner, E.K., 1997. Silicate weathering and climate. In: Ruddiman, W.F. (Ed.), Tectonic Uplift and Climate Change. Plenum Press, New York, pp. 353–365.
Bhatia, M.R., Crook, K.A.W., 1986. Trace element characteristics of graywackes and tectonic discrimination of sedimentary basins. Contributions to Mineralogy and Petrology 92, 181–193.
Bindler, R., 2006. Mired in the past – looking to the future: geochemistry of peat and the analysis of past environmental changes. Global and Planetary Change 53 (4), 209–221.
Braun, J.J., Pagel, M., Herbillon, A., Rosin, C., 1993. Mobilization and redistribution of rees and thorium in a syenitic lateritic profile – a mass-balance study. Geochimica Et Cosmochimica Acta 57 (18), 4419–4434.
Calvert, S.E., Pedersen, T.F., 1996. Sedimentary geochemistry of manganese: implications for the environment of formation of manganiferous black shales. Economic Geology and the Bulletin of the Society of Economic Geologists 91 (1), 36–47.
Danzeglocke, U., Jöris, O., Weninger, B., 2010. CalPal-2007^{online}. <http://www.calpal-online.de/> (accessed 15.10.10).
Ding, Y.H., 1994. Monsoons Over China. Kluwer Academic Publishers, Dordrecht, The Netherlands.
Farmer, J.G., Graham, M.C., Yafa, C., Cloy, J.M., Freeman, A.J., MacKenzie, A.B., 2006. Use of Pb-206/Pb-207 ratios to investigate the surface integrity of peat cores used to study the recent depositional history and geochemical behaviour of inorganic elements in peat bogs. Global and Planetary Change 53 (4), 240–248.
Fralick, P.W., Kronberg, B.I., 1997. Geochemical discrimination of elastic sedimentary rock sources. Sedimentary Geology 113 (1–2), 111–124.
Govil, P., Naidu, P.D., 2011. Variations of Indian monsoon precipitation during the last 32 kyr reflected in the surface hydrography of the Western Bay of Bengal. Quaternary Science Reviews 30, 3871–3879.
Jahn, B.M., Gallet, S., Han, J.M., 2001. Geochemistry of the Xining, Xifeng and Jixian sections, Loess Plateau of China: eolian dust provenance and paleosol evolution during the last 140 ka. Chemical Geology 178 (1–4), 71–94.
Kamenov, G.D., Brenner, M., Tucker, J.L., 2009. Anthropogenic versus natural control on trace element and Sr–Nd–Pb isotope stratigraphy in peat sediments of southeast Florida (USA), similar to 1500 AD to present. Geochimica Et Cosmochimica Acta 73 (12), 3549–3567.
Kempter, H., Gorres, M., Frenzel, B., 1997. Ti and Pb concentrations in rainwater-fed bogs in Europe as indicators of past anthropogenic activities. Water Air and Soil Pollution 100 (3–4), 367–377.
Kronberg, B.I., Nesbitt, H.W., Lam, W.W., 1986. Upper Pleistocene Amazon deep-sea fan muds reflect intense chemical weathering of their mountainous source lands. Chemical Geology 54, 283–294.
Kylander, M.E., Muller, J., Wust, R.A.J., Gallagher, K., Garcia-Sanchez, R., Coles, B.J., Weiss, D.J., 2007. Rare earth element and Pb isotope variations in a 52 kyr peat core from Lynch's Crater (NE Queensland, Australia): proxy development and application to paleoclimate in the Southern Hemisphere. Geochimica Et Cosmochimica Acta 71 (4), 942–960.
Kylander, M.E., Weiss, D.J., Martinez-Cortizas, A., Spiro, B., Garcia-Sanchez, R., Coles, B.J., 2005. Refining the pre-industrial atmospheric Pb isotope evolution curve in Europe using an 8000 year old peat core from NW Spain. Earth and Planetary Science Letters 240 (2), 467–485.
Le Roux, G., Weiss, D., Grattan, J., Givelet, N., Krachler, M., Cheburkin, A., Rausch, N., Kober, B., Shotyk, W., 2004. Identifying the sources and timing of ancient and medieval atmospheric lead pollution in England using a peat profile from Lindow bog, Manchester. Journal of Environmental Monitoring 6 (5), 502–510.
Li, X.H., Liu, Y., Tu, X.L., Hu, G.Q., Zeng, W., 2002. Precise determination of chemical compositions in silicate rocks using ICP-AES and ICP-MS. A comparative study of sample digestion techniques of alkali fusion and acid dissolution. Geochimica 31 (3), 289–294 (in Chinese with English abstract).
Liu, Y., Liu, H.C., Li, X.H., 1996. Simultaneous and precise determination of 40 trace elements in rock samples using ICP-MS. Geochimica 25 (6), 552–558 (in Chinese with English abstract).
Lu, Y.H., 2003. Carbon Isotopes of the Biomarkers in Peats and their Implications for Climate Changes. Thesis for Master's Degree of Zhejiang University.
Martinez-Cortizas, A., Garcia-Rodeja, E., Pontevedra-Pombal, X., Novoa-Munoz, J.C., Weiss, D., Cheburkin, A., 2002. Atmospheric Pb deposition in Spain during the last 4600 years recorded by two ombrotrophic peat bogs and implications for the use of peat as archive. Science of the Total Environment 292 (1–2), 33–44.
Martinez-Cortizas, A., Pontevedra-Pombal, X., Garcia-Rodeja, E., Novoa-Munoz, J.C., Shotyk, W., 1999. Mercury in a Spanish peat bog: archive of climate change and atmospheric metal deposition. Science 284 (5416), 939–942.
McLennan, S.M., 1989. Rare earth elements in sedimentary rocks: influence of provenance and sedimentary processes. In: Lipin, B.R., McKay, G.A. (Eds.), Geochemistry and Mineralogy of Rare Earth Elements. Reviews in Mineralogy, vol. 21, pp. 169–200.
Monna, F., Galop, D., Carozza, L., Tual, M., Beyrie, A., Marembert, F., Chateau, C., Dominik, J., Grousset, F., 2004a. Environmental impact of early Basque mining and smelting recorded in a high ash minerogenic peat deposit. Science of the Total Environment 327 (1–3), 197–214.
Monna, F., Petit, C., Guillaumet, J.P., Jouffroy-Bapicot, I., Blanchot, C., Dominik, J., Losno, R., Richard, H., Leveque, J., Chateau, C., 2004b. History and environmental impact of mining activity in Celtic Aeduan territory recorded in a peat bog (Morvan, France). Environmental Science & Technology 38 (3), 665–673.
Muller, J., Kylander, M., Martinez-Cortizas, A., Wuest, R.A.J., Weiss, D., Blake, K., Coles, B., Garcia-Sanchez, R., 2008. The use of principle component analyses in characterising trace and major elemental distribution in a 55 kyr peat deposit in tropical Australia: Implications to paleoclimate. Geochimica Et Cosmochimica Acta 72 (2), 449–463.
Muller, J., Wust, R.A.J., Weiss, D., Hu, Y., 2006. Geochemical and stratigraphic evidence of environmental change at Lynch's Crater, Queensland, Australia. Global and Planetary Change 53 (4), 269–277.
Nesbitt, H.W., Markovics, G., 1997. Weathering of granodioritic crust, long-term storage of elements in weathering profiles, and petrogenesis of siliciclastic sediments. Geochimica Et Cosmochimica Acta 61 (8), 1653–1670.
Nesbitt, H.W., Markovics, G., Price, R.C., 1980. Chemical processes affecting alkalis and alkaline earths during continental weathering. Geochimica Et Cosmochimica Acta 44, 1659–1666.
Nesbitt, H.W., Young, G.M., 1982. Early proterozoic climates and plate motions inferred major element chemistry of lutites. Nature 299, 715–717.
Pedersen, T.F., Price, N.B., 1982. the geochemistry of manganese carbonate in panama basin sediments. Geochimica Et Cosmochimica Acta 46 (1), 59–68.
Postma, D., 1981. Formation of siderite and vivianite and the pore-water composition of a recent bog sediment in Denmark. Chemical Geology 31 (3), 225–244.
Postma, D., 1982. Pyrite and siderite formation in brackish and fresh-water swamp sediments. American Journal of Science 282 (8), 1151–1183.
Roos-Barraclough, F., Martinez-Cortizas, A., Garcia-Rodeja, E., Shotyk, W., 2002. A 14 500 year record of the accumulation of atmospheric mercury in peat: volcanic

signals, anthropogenic influences and a correlation to bromine accumulation. Earth and Planetary Science Letters 202 (2), 435–451.
Rudnick, R.L., Gao, S., 2003. Composition of the continental crust. In: Rudnick, R.L. (Ed.), Treatise on Geochemistry, The Crust, vol. 3. Elsevier Ltd., pp. 1–64.
Schroeder, J.O., Murray, R.W., Leinen, M., Pflaum, R.C., Janecek, T.R., 1997. Barium in equatorial Pacific carbonate sediment: terrigenous, oxide, and biogenic associations. Paleoceanography 12 (1), 125–146.
Shotyk, W., Goodsite, M.E., Roos-Barraclough, F., Givelet, N., Le Roux, G., Weiss, D., Cheburkin, A.K., Knudsen, K., Heinemeier, J., Van der Knaap, W.O., Norton, S.A., Lohse, C., 2005. Accumulation rates and predominant atmospheric sources of natural and anthropogenic Hg and Pb on the Faroe Islands. Geochimica Et Cosmochimica Acta 69 (1), 1–17.
Shotyk, W., Weiss, D., Appleby, P.G., Cheburkin, A.K., Frei, R., Gloor, M., Kramers, J.D., Reese, S., Van der Knaap, W.O., 1998. History of atmospheric lead deposition since 12,370 C-14 yr BP from a peat bog, Jura Mountains, Switzerland. Science 281 (5383), 1635–1640.
Shotyk, W., Weiss, D., Kramers, J.D., Frei, R., Cheburkin, A.K., Gloor, M., Reese, S., 2001. Geochemistry of the peat bog at Etang de la Gruere, Jura Mountains, Switzerland, and its record of atmospheric Pb and lithogenic trace metals (Sc, Ti, Y, Zr, and REE) since 12,370 C-14 yr BP. Geochimica Et Cosmochimica Acta 65 (14), 2337–2360.
Singh, R.P., Tripathi, R.D., Sinha, S.K., Maheshwaril, R., Srivastava, H.S., 1997. Response of higher plants to lad contaminated environment. Chemosphere 34, 2467–2473.
Wang, B., Lin, Ho, 2002. Rainy season of the Asian-Pacific summer monsoon. Journal of Climate 15 (4), 386–398.
Wang, Y.J., Cheng, H., Edwards, R.L., Kong, X.G., Shao, X.H., Chen, S.T., Wu, J.Y., Jiang, X.Y., Wang, X.F., An, Z.S., 2008. Millennial- and orbital-scale changes in the East Asian monsoon over the past 224,000 years. Nature 451 (7182), 1090–1093.
Wei, G.J., Li, X.H., Liu, Y., Shao, L., Liang, X.R., 2006. Geochemical record of chemical weathering and monsoon climate change since the early Miocene in the South China Sea. Paleoceanography 21 (4), PA4214. http://dx.doi.org/10.1029/2006PA001300.
Wei, G.J., Liu, Y., Li, X.H., Shao, L., Fang, D.Y., 2004. Major and trace element variations of the sediments at ODP Site 1144, South China Sea, during the last 230 ka and their paleoclimate implications. Palaeogeography Palaeoclimatology Palaeoecology 212 (3–4), 331–342.
Weiss, D., Shotyk, W., Appleby, P.G., Kramers, I.D., Cheburkin, A.K., 1999. Atmospheric Pb deposition since the industrial revolution recorded by five Swiss peat profiles: Enrichment factors, fluxes, isotopic composition, and sources. Environmental Science & Technology 33 (9), 1340–1352.
Weiss, D., Shotyk, W., Cheburkin, A.K., Gloor, M., Reese, S., 1997. Atmospheric lead deposition from 12,400 to Ca. 2,000 yrs BP in a peat bog profile, Jura mountains, Switzerland. Water Air and Soil Pollution 100 (3-4), 311–324.
Wust, R.A.J., Bustin, R.M., 2003. Opaline and Al–Si phytoliths from a tropical mire system of West Malaysia: abundance, habit, elemental composition, preservation and significance. Chemical Geology 200 (3–4), 267–292.
Zhao, K., Wang, Y.J., Edwards, R.L., Cheng, H., Liu, D.B., 2010. High-resolution stalagmite $\delta^{18}O$ records of Asian monsoon changes in central and southern China spanning the MIS 3/2 transition. Earth and Planetary Science Letters 298 (1–2), 191–198.